KfK 5091
Dezember 1992

# Comparison of Results of Two-Phase Fluid Dynamics Codes and Sloshing Experiments

C.-D. Munz, W. Maschek
Institut für Neutronenphysik und Reaktortechnik
Projekt Nukleare Sicherheitsforschung

Kernforschungszentrum Karlsruhe

KERNFORSCHUNGSZENTRUM KARLSRUHE

Institut für Neutronenphysik und Reaktortechnik

Projekt Nukleare Sicherheitsforschung

KfK 5091

# Comparison of Results of Two-Phase Fluid Dynamics Codes and Sloshing Experiments

C.-D. Munz, W. Maschek

Kernforschungszentrum Karlsruhe GmbH, Karlsruhe

Kernforschungszentrum Karlsruhe GmbH
Postfach 3640, 7500 Karlsruhe 1

ISSN 0303-4003

**This report is dedicated to**
**our good friend Klaus Küfner**
**who passed away much too early**

**Abstract**

The phenomenon of motion of liquids in containers, referred as "sloshing", has been a subject of investigation for many years.

Liquid sloshing phenomena can be triggered e.g. by seismic effects in water reservoirs (dams) or oil tanks. It can also be initiated by moving of the liquid container itself as in the case of supertankers or large liquid propellant rockets. Characteristically the sloshing in these systems is a wave motion from one side of the container to the other or an azimuthal motion.

In the framework of core disruptive accident simulation in a liquid metal fast breeder reactor (LMFBR) another type of sloshing manifests. Under specific pessimistic assumptions the reactor core melts and a large whole core liquid fuel pool confined by blockages emerges in the socalled transition phase. A local fuel compaction may trigger a mild nuclear excursion in this pool. The following energy deposition leads to a pressure build-up in the core center which pushes the liquid fuel towards the core periphery. Driven by gravity the fuel sloshes back towards the core center and piles up in a neutronically critical or even supercritical configuration. This "centralized sloshing" can lead to energetic nuclear power excursions.

Because of the importance of the sloshing phenomenon in accident analyses the used simulation codes should be able to describe this process adequately.
Three codes were tested in this framework: SIMMER-II, AFDM and IVA3. The SIMMER-II and the AFDM codes are suitable for the simulation of accident phenomena in the LMFBR area. Both codes must be able to describe sloshing with good accuracy because in the specific accident phenomenology the fluid motion is coupled with a neutronic reactivity feedback which can lead to a nuclear excursions. The IVA3 code is used for accident simulation in the light water reactor (LWR) field - especially for pressurized water reactors (PWRs). Sloshing phenomena which determine the local fuel accumulation may occur in the case when the fuel melts down into the reactor cavity (the neutronic effects are of minor importance).

An extensive literature research showed that no experimental information was available on this specific type of "centralized sloshing". Therefore it was decided to set up own simple experiments to investigate both the phenomenon of centralized sloshing and to provide experimental data for the benchmark exercise with the SIMMER-II, AFDM and IVA3 codes. The centralized sloshing of fluids can be regarded as a good test for numerical schemes as both smooth but compact wave packages and sharp fluid peaks characterize the flow.

Results of this exercise will also influence the future SIMMER-III development which is a common enterprise between the Power Reactor and Nuclear Fuel Development Corporation (PNC) and the European Partners, Kernforschungszentrum Karlsruhe (KfK); Atomic Energy Authority-Technology (AEA-T) and Commissariat á l'Energie Atomique (CEA).

## Vergleich der Resultate von Zweiphasenströmungs-Codes und Schwappexperimenten

## Zusammenfassung

Das Schwappen von Flüssigkeiten in Behältern wird seit vielen Jahren intensiv untersucht.
Solche Schwappbewegungen können z.B. durch seismische Aktivität bei Staudämmen oder in Öltanks ausgelöst werden. Die Bewegung des Behälters selbst - wie im Falle von Supertankern oder Flüssigkeitsraketen - kann ebenso Schwappbewegungen auslösen. Die Schwappbewegung verläuft in diesen Fällen jeweils von einer zur anderen Seite des Containers bzw. es können azimutale Bewegungsvorgänge auftreten.

Im Rahmen der Simulation von Kernzerstörungsunfällen bei Schnellen Brutreaktoren kann sich eine spezielle Form dieses Flüssigkeitsschwappens ausbilden.
Unter bestimmten pessimistischen Annahmen kann der Kern zusammenschmelzen und sich ein großer Brennstoffpool bilden, der von Blockaden umschlossen ist. Lokale Brennstoffkompaktionen können eine milde Exkursion auslösen, die wiederum zu einer Schwappbewegung des flüssigen Brennstoffes führt.

Der flüssige Brennstoff wird dabei vom Zentrum weg an die Peripherie des Cores getrieben, kehrt unter Gravitationswirkung wieder zum Zentrum zurück und kompaktiert zu einer neutronisch kritischen bzw. überkritischen Konfiguration. Dieses "zentralisierte Schwappen" kann dabei energetische Leistungsexkursionen auslösen.

Wegen der Wichtigkeit dieser Schwappphänomene bei der Beschreibung von Störfallabläufen müssen diese Phänomene von den Simulationscodes hinreichend genau beschrieben werden. In diesem Rahmen wurden drei Codes getestet: SIMMER-II, AFDM und IVA3.
Der SIMMER-II und AFDM Code sind Codes zur Beschreibung des Störfallablaufes bzw. von Störfallphänomenen im Bereich der Schnellbrütersicherheit.
Beide Codes sollten Schwappphänomene mit guter Genauigkeit beschreiben können, da die Fluidbewegung mit neutronischen Reaktivitätseffekten gekoppelt ist. Der IVA3 Code wird zur Simulation von Störfallabläufen bei Leichtwasserreaktoren - vor allem Druckwasserreaktoren - eingesetzt. Schwappphänomene können dabei auftreten, wenn der Brennstoff in die Reaktorgrube durchschmilzt. (Die neutronische Rückwirkung ist dabei von geringer Bedeutung.)

Eine intensive Literaturstudie zeigte, daß keine experimentellen Informationen über die spezielle Form des "zentralisierten Schwappens" vorliegen. Es wurden daher bei KfK einfache Experimente durchgeführt, die einen tieferen Einblick in die Phänomenologie geben sollten und darüberhinaus als Benchmarks für die numerische Simulation mit SIMMER-II, AFDM und IVA3 dienen konnten.
Dieses "zentralisierte Schwappen" kann als guter Test für numerische Methoden angesehen werden, da sowohl kompakte Wellenpakete als auch spitze Flüssigkeitsberge während der Bewegung auftreten.

Die Ergebnisse dieser Untersuchungen beeinflussen auch die SIMMER-III Entwicklung, die in einem gemeinsamen Unternehmen der Power Reactor and Nuclear Fuel Development Corporation (PNC) und den Europäischen Partnern, dem Kernforschungszentrum Karlsruhe (KfK), der Atomic Energy Authority-Technology (AEA-T) und dem Commissariat á l'Energie Atomique (CEA) durchgeführt wird.

Table of Contents

## 1. Introduction

The phenomenon of motion of liquids in containers, referred as "sloshing", has been a subject of interest to many investigators and engineers (for reviews see /1 - 3/).

Liquid sloshing phenomena can be triggered e.g. by seismic effects in water reservoirs (dams), oil tanks or large pool reactors. It can also be initiated by moving of the liquid container itself as in the case of supertankers of liquified natural gas (LNG) ships and large liquid propellant rockets. A large number of publications is available on this widespread natural phenomenon "sloshing". The emphasis of all experimental and theoretical investigations is mainly put on the dynamic effects (pressure loads) of the moving and impacting waves and on stability questions (spacecraft). Characteristically the sloshing in these systems is a wave motion from one side of the container to the other or an azimuthal motion.

In the framework of core disruptive accident simulation in a liquid metal fast breeder reactor (LMFBR) another type of sloshing manifests /4 - 7/. Under specific pessimistic assumptions the reactor core melts and a large whole core liquid fuel pool confined by blockages (frozen fuel and blanket structures) emerges in the socalled transition phase /8/. A local fuel compaction may trigger a mild nuclear excursion in this pool. The following energy deposition leads to a pressure build-up in the core center which pushes the liquid fuel towards the core periphery. Driven by gravity the fuel sloshes back towards the core center and piles up in a neutronically critical or even supercritical configuration. This "centralized sloshing" /9/ which is schematically depicted in Fig. 1.1 can lead to energetic nuclear power excursions and the conditions and phenomena of these processes are therefore studied extensively.

The main interest in this research area is not related to the dynamic effects of the sloshing process as the impact of the sloshing liquid on the container walls but more to its inherent structure as velocity of compaction, sharpness of the wave front and stability of the converging waves as these issues define the resulting neutronic reactivity ramp rates by the compacting fuel. Because of the importance of the sloshing phenomenon in accident analyses the used simulation codes should be able to describe this process adequately.

Three codes were tested in this framework: SIMMER-II /10/, AFDM /11/ and IVA3 /12 - 14/. The SIMMER-II code /10/ and the AFDM code /11/ (which can be regarded as a basis for the future SIMMER-III development a joint undertaking of PNC, KfK, AEAT and CEA) are codes for the description of accident phenomena in the LMFBR area. Both codes must be able to simulate sloshing with good accuracy because in the specific accident phenomenology the fluid motion is coupled with neutronic feedback which can lead to a nuclear excursion. The IVA3 code /10/ is used for accident simulation in the light water reactor (LWR) field - especially for pressurized water reactors (PWRs). Sloshing phenomena which determine the local fuel accumulation may occur in the case when the fuel melts down into the reactor cavity (the neutronic effects are of minor importance).

It should be mentioned that all three codes are two phase codes with no specific tracking of the fluid surface. They are based on volume and time averaged equations. By this and the inherent numerical diffusion of the codes the free surface of the moving liquid is smeared out to a certain extent. This represents a general difficulty in describing sloshing phenomena by numerical calculations.
The main interest in this study was focussed on the question if the wave packages (the mass centroid) stay together or are diffused out by numerical dissipation inherent in the codes.

As a detailed code description of all three codes can be found in the above mentioned literature only a short description of SIMMER-II, AFDM and IVA3 is given.

In the SIMMER II Code a set of time dependent, two dimensional equations for the densities, velocities and internal energy is solved. The numerical approximation of the convective terms is performed in an explicit way using first order donor-cell differencing while the pressure terms are handeled implicitely by central differencing. By that a time step restriction based on the velocity of the fast pressure waves is omitted. The mesh is organized in a staggered way: density pressure, and temperatures are defined at cell centers while the velocities are defined at the cell interfaces. The transport equations for the velocities are solved on a grid shifted half a space step.

The AFDM-Code (Advanced Fluid Dynamics Code) has been designed as a test-code with improved numerical approximation of hydrodynamics as well as improved mathematical modelling of the exchange terms. The set of equations and their approximation used in AFDM are formulated in conservation form to

retain the integral conservation as far as possible. The numerical method of SIMMER-II for the hydrodynamic part has been extended in AFDM to second order accuracy in time and space.

The IVA3-Code is a time-dependent three dimensional multiphase code and is based on a quite similar numerical approximation technique as SIMMER II, but the energy equation is replaced by the equation of conservation of entropy. By that, the set of equations becomes simpler. Because the conservation of entropy is not valid in the vicinity of shock waves, we expect for IVA3 problems with shock waves in the gas phase and with the integral conservation of the energy. But these disadvantageous properties should not play a big role in the sloshing motion considered in this paper.

An extensive literature research showed that no experimental information was available on this specific type of "centralized sloshing" for comparison with the numerical results. Therefore it was decided to set up our own simple experiments to investigate both the phenomenon of centralized sloshing and to provide experimental data for the benchmark exercise with the SIMMER-II, AFDM and IVA3 codes. A detailed description of these experiments is given in /16/. The centralized sloshing of fluids can be regarded as a good test for numerical schemes as both smooth but compact wave packages and sharp fluid peaks characterize the flow.

Results of this exercise will also influence the future SIMMER-III development which is a common enterprise between PNC and the European Partners KfK, AEA-T and CEA.

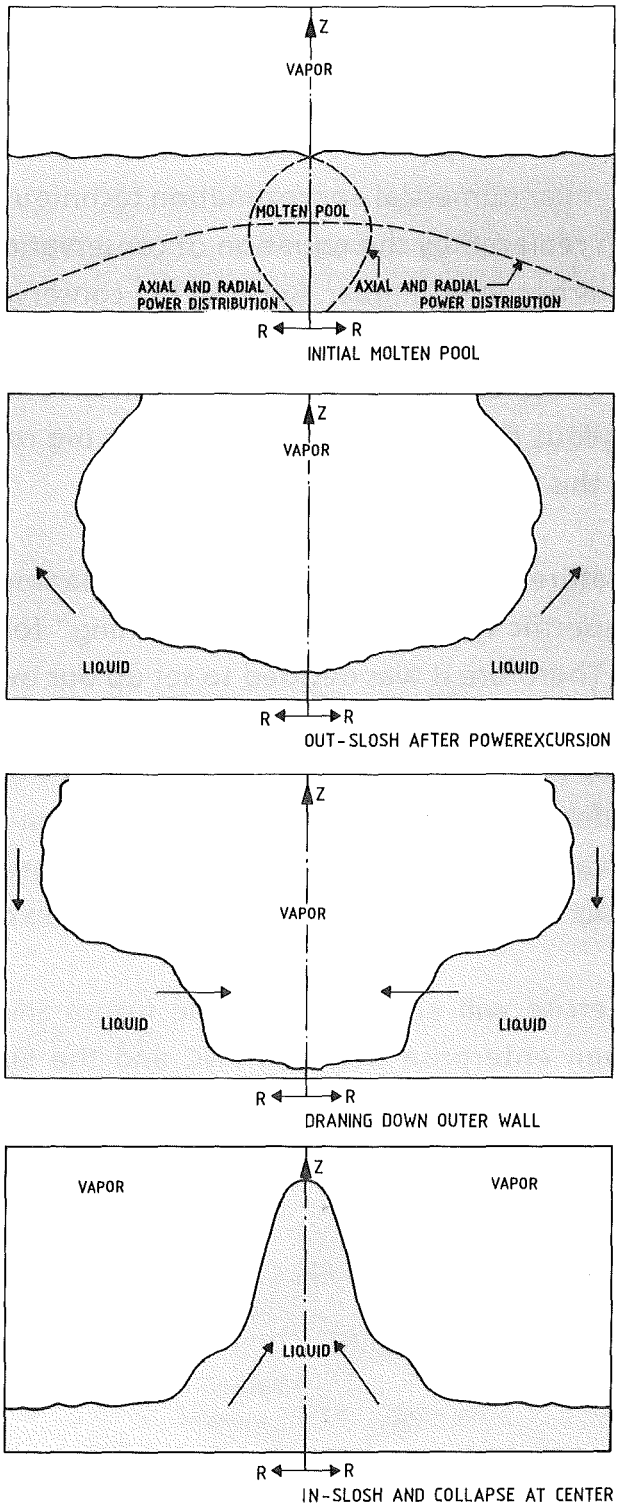


Figure 1.1: Schematic representation of liquid fuel sloshing in a container

## 2. Liquid Sloshing Problems

Two cases of typical sloshing problems are considered in this exercise. For both, a cylindrical container is divided into two concentric parts by a cylindrical diaphragm. In the first case only the inner cylinder contains water of a certain depth, the outer cylinder contains air. A (r,z)-diagram of this situation is shown in Figure 2.1. Four problems with different diameters of the cylindrical diaphragm and different water depths are considered. These problems are called the "**(cylindrical) dam break problem**". The other case is defined as the "**(cylindrical) water step problem**". In this latter configuration both - the inner and outer cylinder - contains water. The depth of the water in the inner cylinder is higher than in the outer one (see Fig. 2.2).

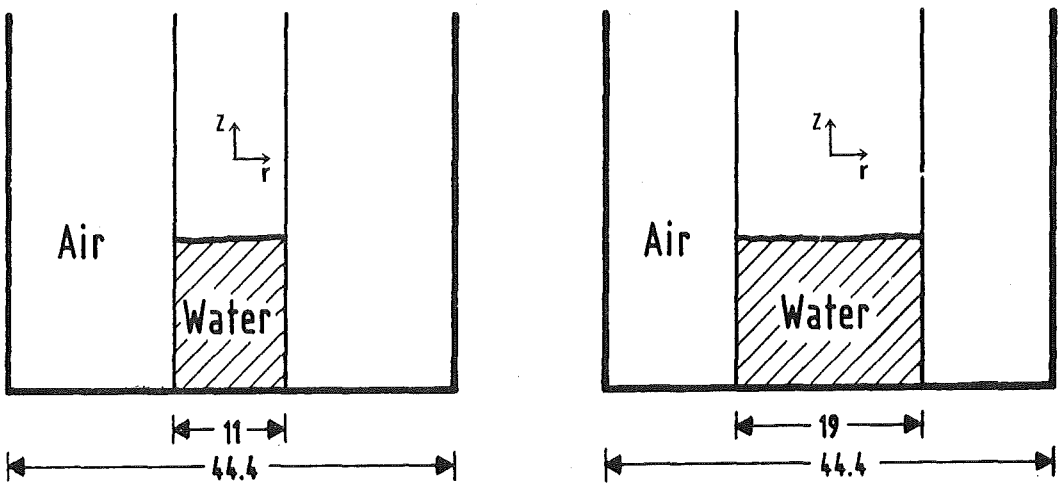


Figure 2.1: Dam break problem in the (r,z)-plane

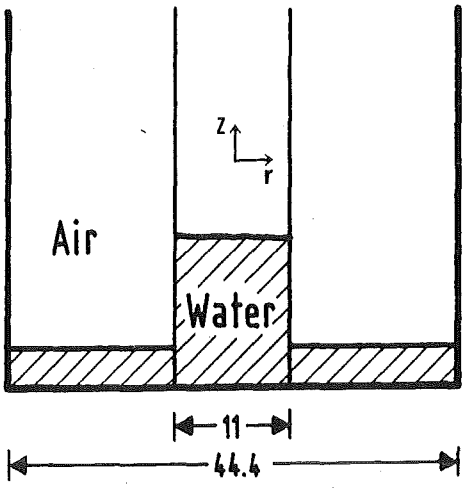


Figure 2.2: Water step problem in the (r,z)-plane

At time t = 0 the diaphragm is supposed to be removed suddenly and the water and air are set in motion. A water wave will flow outwards and finally reaches the outer cylinder, it is reflected and the reversal wave travels towards the center. This cylindrical water wave converges and produces a high water peak in the center. By this collapse at the axis the water wave is again reflected and moves outwards. The amplitude of this wave is now smaller due to the viscous forces.

Five test problems are considered: two dam break problems with a small inner water cylinder (left diagram in Figure 2.1) and different water depths, two problems with a bigger inner water cylinder (right diagram in Figure 2.1) and one water step problem (Figure 2.2). The different values for the diameter of the diaphragm and the water depths are given in Table 2.1.

| Test problem | inner diameter [cm] | water depth inner cylinder [cm] | water depth outer cylinder [cm] |
|---|---|---|---|
| 1 | 11 | 10 | 0 |
| 2 | 11 | 20 | 0 |
| 3 | 19 | 10 | 0 |
| 4 | 19 | 20 | 0 |
| 5 | 11 | 20 | 5 |

Table 2.1: Parameters specification for test problems 1 - 5

The typical experimental set-up shown in Fig. 2.3 modelled a cylindrical dam break problem (and similar a fluid step problem) basically using two cylindrical containers.

In the experiments a central water column with different heights and diameters (11 cm and 19 cm) is released from a small cylindrical plexiglas container which is shot upwards with a speed of ~ 3 m/s. This velocity is sufficient to obtain the free standing water column as displayed in Fig. 2.4. The motion was followed by video- and high speed camera. In this way measured and calculated sloshing heights and velocities of reassembling liquids could be directly compared (see /9, 16/).

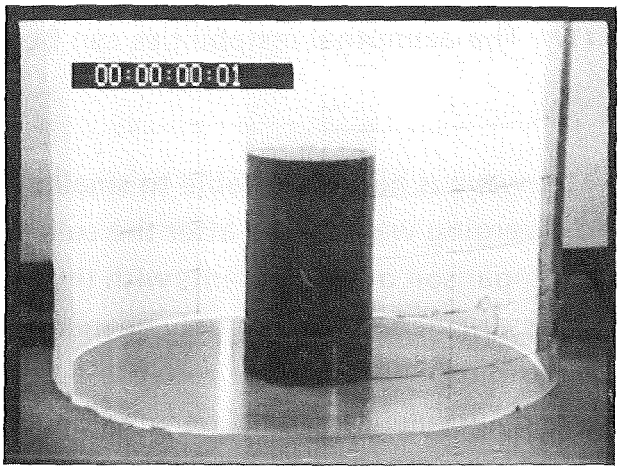


Figure 2.3: Typical experimental set up

| Test problem | $t_1$ [sec] | $t_2$ [sec] | maximal $h_{sl}$ [cm] | $t_3$ [sec] | maximal $h_{co}$ [cm] |
|---|---|---|---|---|---|
| 1 | 0.21 ± 0.02 | 0.36 ± 0.02 | 9.0 ± 1.0 | 0.84 ± 0.04 | 25.0 ± 5 |
| 2 | 0.20 ± 0.02 | 0.42 ± 0.02 | 16.0 ± 1.0 | 0.88 ± 0.04 | 40.0 ± 5 |
| 3 | 0.16 ± 0.02 | 0.34 ± 0.02 | 14.0 ± 1.0 | 0.80 ± 0.04 | 40.0 ± 6 |
| 4 | 0.15 ± 0.02 | 0.40 ± 0.02 | 22.0 ± 1.0 | 0.82 ± 0.04 | 60.0 ± 10 |
| 5 | - | 0.36 ± 0.02 | 11.0 ± 1.0 | 1.24 ± 0.04 | 50.0 ± 5 |

$h_{sl}$: sloshing height at outer cylinder wall [cm]
$h_{co}$: collapse height [cm]
$t_1$: time of arrival at outer cylinder wall [sec]
$t_2$: time of maximal sloshing height at the wall [sec]
$t_3$: time of maximal collapse height [sec]

Table 2.2: Experimental results of the sloshing experiments

A general point of interest is that the centralized in-sloshes from the converging water waves are highly unstable and easily disturbed. This is in accordance with known physical principles /17/. The azimuthal instabilities can be clearly seen in Fig. 2.5.

Because the converging water wave is highly unstable to small perturbations of symmetry, the reflected and diverging water wave after the collapse is no longer radially symmetric. Hence, a comparison of experiments with the radially symmetric numerical or analytical results (r,z geometry) can only be made up to the point of the collapse. Furthermore, during and after the collapse a precise numerical modelling of viscous forces and turbulence should become important, while in the initial stage this should not have such a large influence. Hence to compare the two-dimensional numerical results with the experiments, one is mostly interested in the first initial sloshing phases up to the time of central collapse. Besides the structure of the flow the favourable values for comparison are the times, when the water will reach the confining outer cylinder wall, the height and time of maximal sloshing at the cylinder wall and the time when the central collapse starts. Also the time and the maximal height of the central collapse are listed. These quantities have the greatest experimental uncertainty* (Tab. 2.2). The measured quantities were sufficiently accurate for discriminating e.g. whether the first order SIMMER-II or IVA-3 calculations give an adequate simulation of the sloshing process or whether a second order scheme is required. A sequence of pictures showing the main stages of the experiments according to Test Problem 2, can be seen in Figure 2.4: the initial stage, the sloshing at the outer cylinder wall and the centralized sloshing.

For test problem 5 the specific combination of water heights in the inner and outer container lead to an interesting oscillating system by the interference of the released water column with the outer water ring. The experimental results are displayed in Fig. 2.6. A first inward slosh only leads to a water hump, whereas the highly peaked inward slosh (similar to the dam break) comes only after an intermediate second outward slosh. The height of the second peak is given in Table 2.2. With a lower or higher water depth in the outer container, the high peak after the first outward slosh reemerges. Note that the arrival time of the wave at the outer wall cannot be clearly determined for problem 5. Before a sur-

* The instabilities can easily lead to severe sideward distortions of the central sloshing peak and these cases were not taken into account in Tab. 2.1.

face wave arrives at the outer cylinder wall, the outer level of the water increases because of waves in the "deep" water. The starting point of these mechanisms is difficult to observe, and hence, we decided in this case to drop the arrival time $t_1$ in Table 2.2.

For the maximum sloshing height and the time of maximum collapse only approximate values are given. The most upper part in the central water peak is split up in a stream of droplets and a certain height is difficult to determine. In our cases only the continuous liquid stream was assumed as peak (for details see /16/). The accuracy of the measured sloshing heights were however by far sufficient to assess the adequacy of the used numerical schemes.

These results are compared with numerical calculations by AFDM, SIMMER II and IVA3. In all three codes the symmetry according to the angle are imposed. Both AFDM and SIMMER II are two-dimensional codes using r,z-coordinates. IVA3 is a three-dimensional code but is used here in a two-dimensional manner. The assumption of total symmetry is violated in our experiments and in the real situation for the converging water wave and the central sloshing due to instabilities as mentioned above. Hence, the numerical results by imposing symmetry should overestimate the central sloshing heights obtained in the experiments.

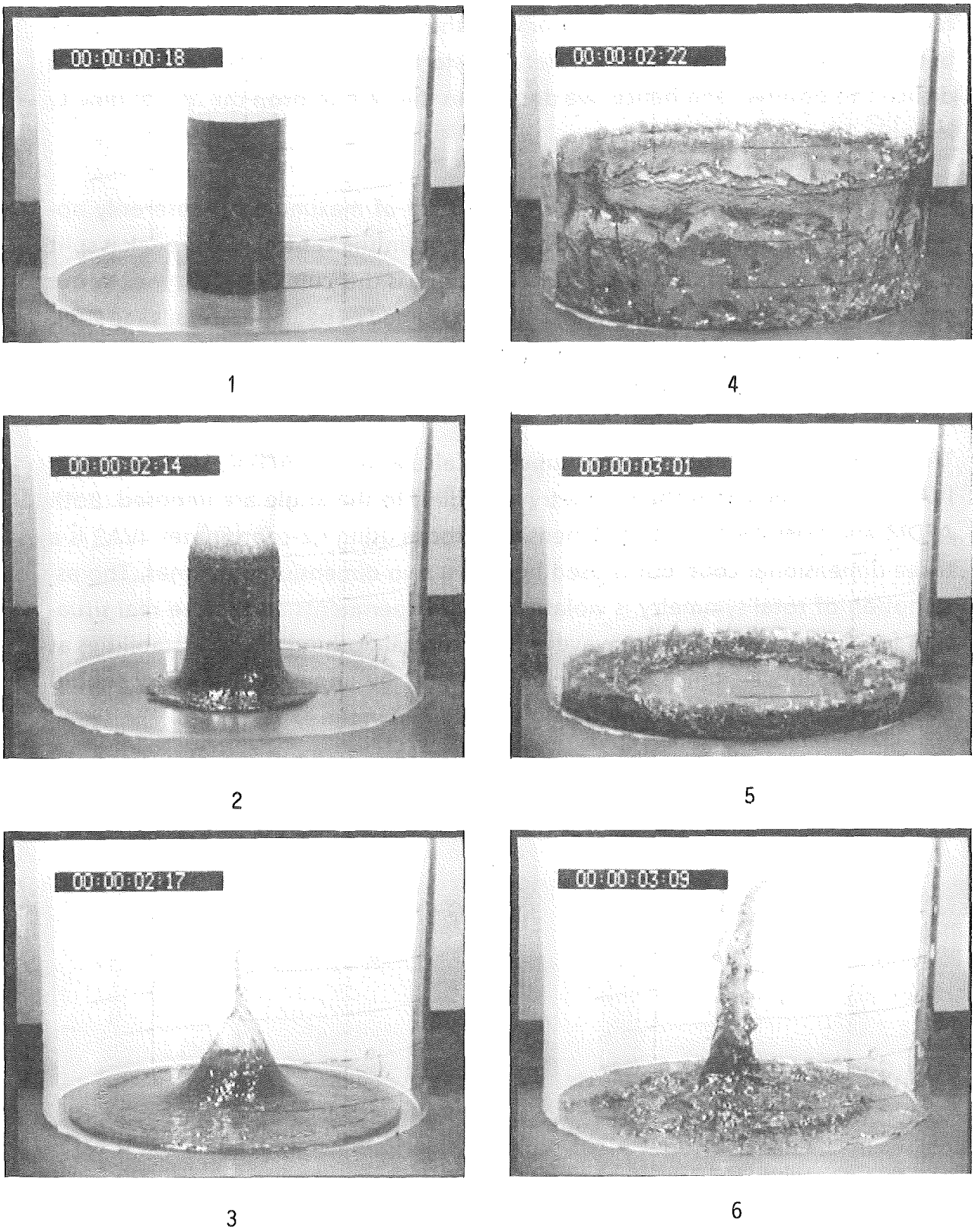


Figure 2.4: Experimental results for Test Problem 2

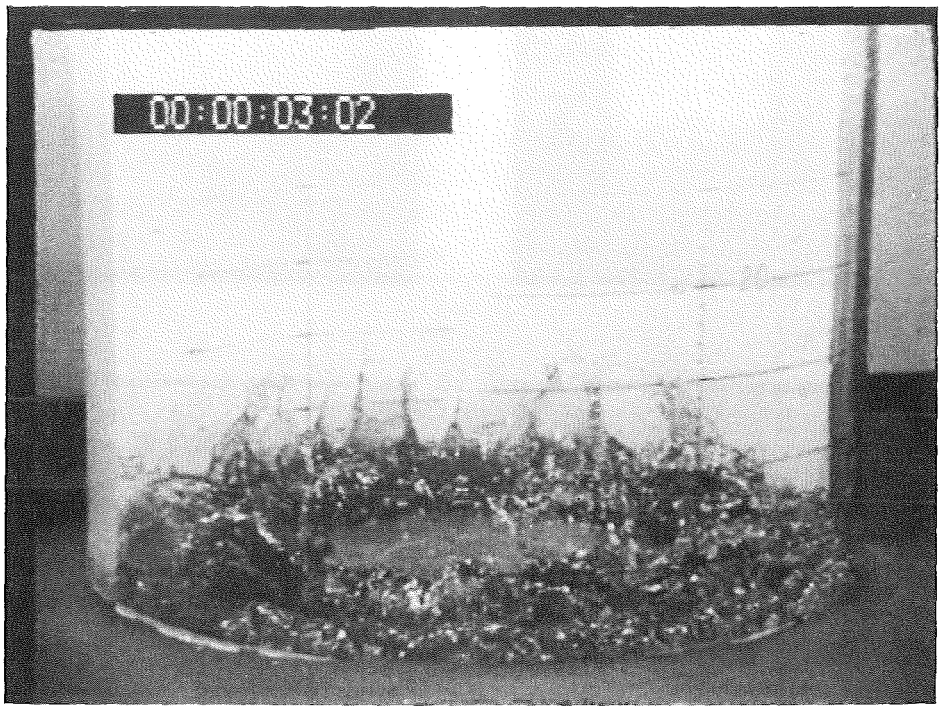


Figure 2.5: Experimental results for Test Problem 2: Instabilities of the converging water wave

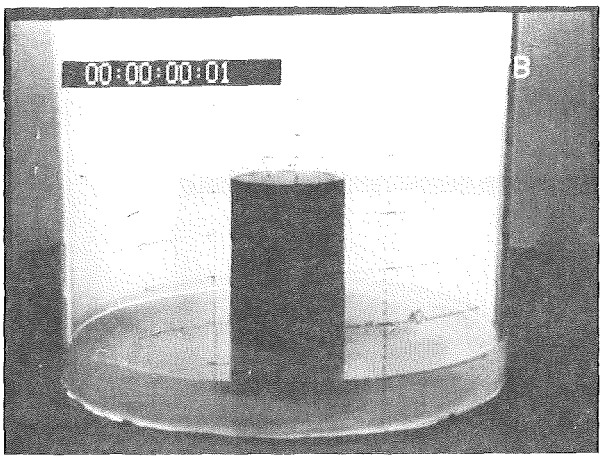


1

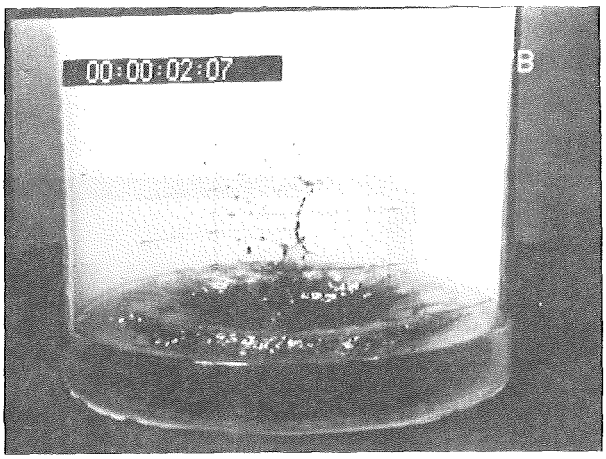


2

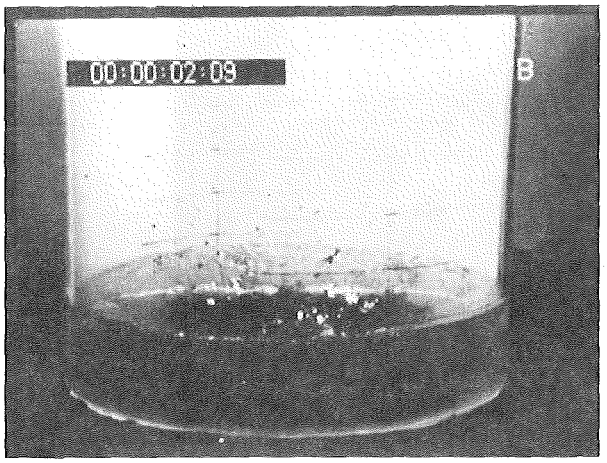


3

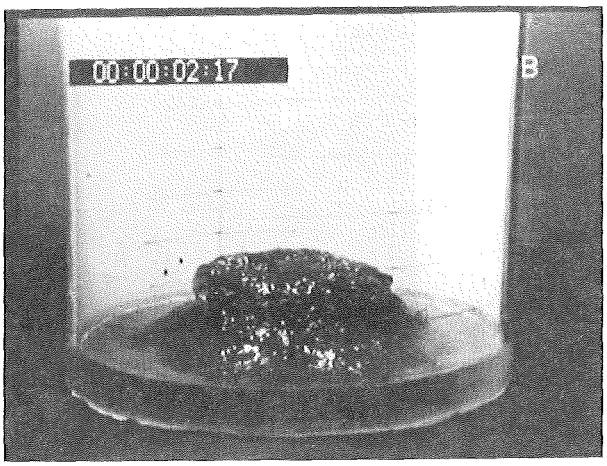


4

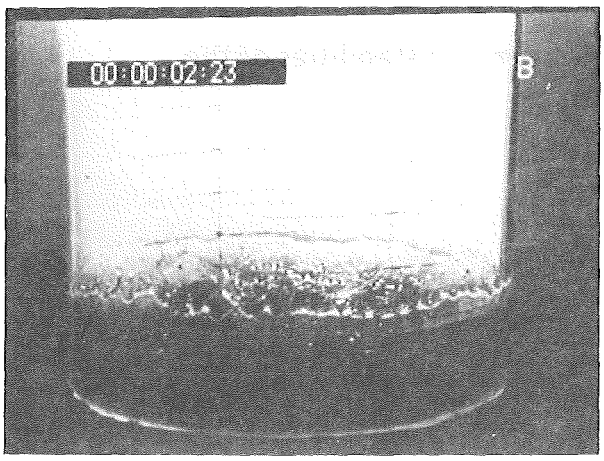


5

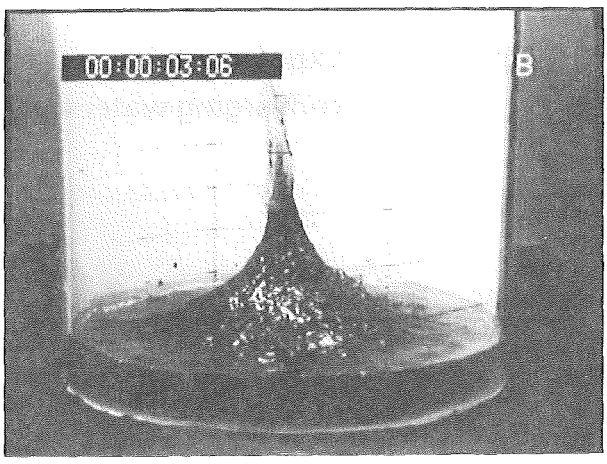


6

Figure 2.6: Experimental results for the water step problem (Test Problem 5)

## 3. Analytical Results

The shallow water approximation may give a first impression about the structure of the solution. This is a first order approximation of the fluid dynamic equations under the assumption that the water depth of the problem is much smaller than its length scale. This assumption is not satisfied by our problems. Hence, one has to be very careful in a quantitative or qualitative comparison of shallow water solutions with the experimental results, but they give insight into the initial structure of the solution. We remark that the names of the test problems such as dam break problem may lead to confusion within this context, because the practical flow after breaking a dam is a typical application of the shallow water equations (see /17/). Nevertheless, the shallow water solutions should be of use, because in plane symmetry the shallow water equations admit simple analytical solutions based on the theory of characteristics (see e.g. /17/). The situation of the dam break and water step problem in plane symmetry is sketched in the Figure 3.1. The upper diagrams show the initial data. The diagrams in the middle show the time evolution of fluid flow by drawing the characteristics in the (x,t)-plane. The diagrams below show the solution at a fixed time. The spatial variable r is replaced by x to remember that these considerations are valid in cartesian coordinates.

For the dam break problem a rarefaction wave occurs which moves to the right and left with propagation rate 2 $c_o$ and $c_o$, respectively. This velocity depends on the gravity and water depth: $c_o = \sqrt{gh_o}$. A typical solution at a fixed time is shown in the last diagram. In the cylindrical case the structure of the solution is quite similar, but the characteristics are no longer straight lines. The characteristics to the right become convex curves due to the geometrical effects which means that the velocity decreases. The velocity to the left increases by the convergence of the geometry. In the water step problem a rarefaction wave travels to the left and a discontinuous water wave similar to a outwards travelling wave moves to the right with velocity s. Between rarefaction wave and shock wave occurs a state of constant water depth. In the cylindrical case the characteristics are curved lines and analogously to the dam break problem the outwards travelling waves become slower, and the wave travelling towards the axis becomes faster. Due to the curved characteristics the solution can no longer be solved analytically in a simple way. Because the shallow water solutions are no good candidates for a quantitative comparison with numerical results for our test problems, it was not tried to solve the shallow water equations in (r, z) coordinates numerically.

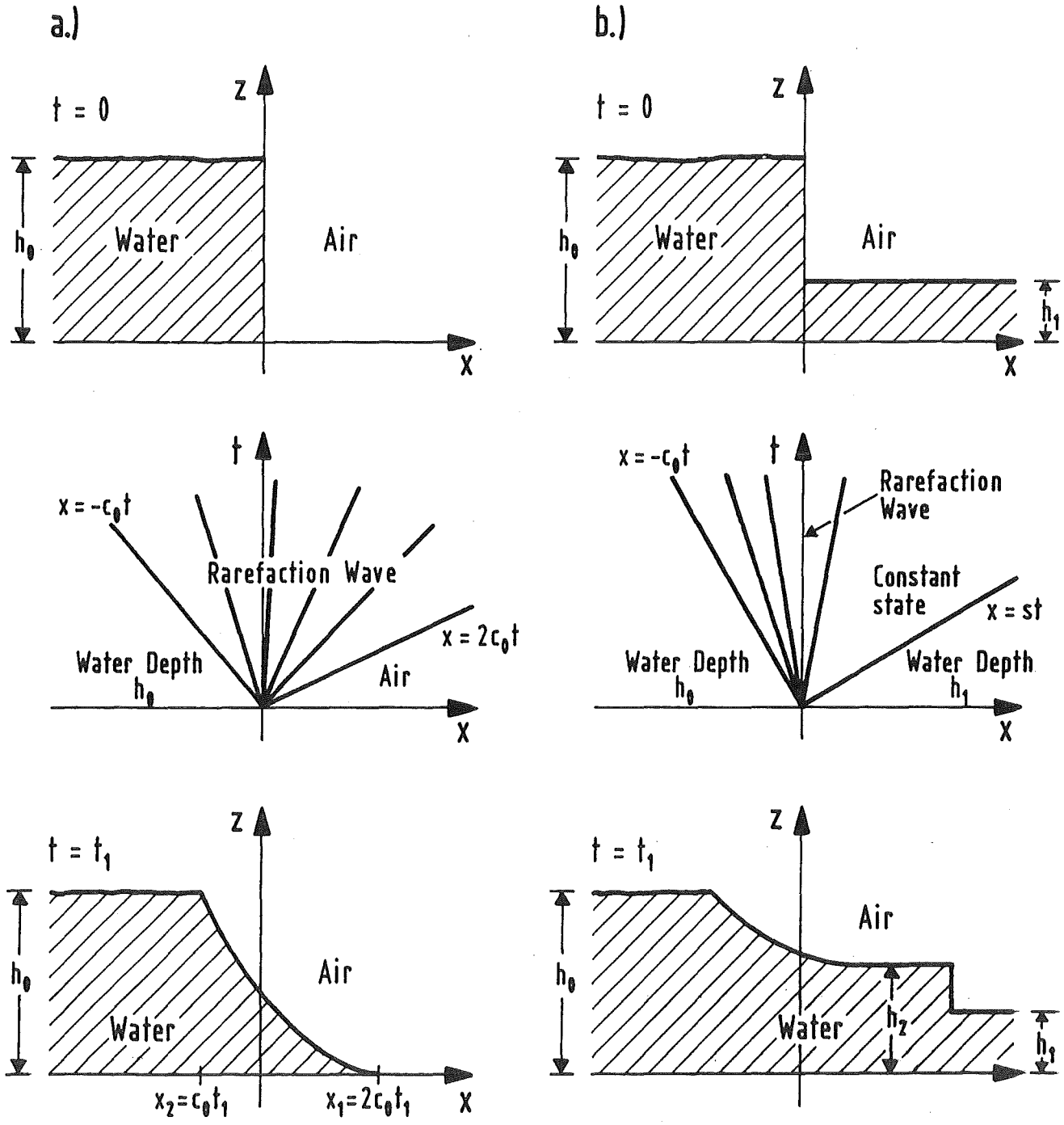


Figure 3.1: Shallow water solution of the a.) dam break problem and b.) water step problem in plane symmetry

## 4. Numerical Model and Basic Input Data

For the calculations, presented here, the Version AA of the AFDM-Code was used, which is implemented at KfK. In that version changes of the code have been taken into account up to the 10th of August 1989. In the first series of calculations the KQQM1 ON option (The simplified method for calculating momentum and heat transfer was chosen). In a second series the KQQM2 ON option (i.e. the standard models for momentum and heat transfer) was used. For details see reference /11/.
In a first series of calculations a grid with 23 x 43 grid zones is used. The axial length of the grid zones are determined in such a way that the diaphragm coincides with a grid zone boundary and that the grid becomes nearly uniform with stepsizes $\Delta r = 1$ cm, $\Delta z = 1$ cm. For instance, for Test Problem 1 we choose $\Delta r_i = 1.0$ cm for $i = 1 - 5$, $\Delta r_i = 0.5$ cm for $i = 6, 7$, $\Delta r_i = 1.0$ cm for $i = 8 - 21$ and $\Delta r_i = 1.1$ cm for $i = 22,23$, $\Delta z = 1$ cm for $j = 1 - 43$. In a second series of calculations the grid was refined up to 46 x 86 grid zones by dividing the grid zones into halves. The other parameters are kept fixed.

For the SIMMER comparative calculations both the SIMMER-II Versions 9 and 10 were used. All calculations were done on a similar grid as the AFDM calculations with 23 x 43 grid zones and the above mentioned distances for $\Delta r$ and $\Delta z$. No calculations with mesh refinement have been performed with SIMMER. Some parametric studies have been performed with SIMMER to estimate the influence of taking into account viscous terms in the momentum equation (IVIS = 1), the influence of the drag coefficient, the slip between liquid and gas etc. As expected these quantities did not have a significant influence on the sloshing motion simulation with SIMMER.

The same grid has been also used by the IVA3 comparative calculations: 23 x 43 grid zones with the above mentioned distances for $\Delta r$ and $\Delta z$. No calculations with mesh refinement have been performed with IVA3.

# 5. AFDM-Results

## 5.1 KQQM1-Option

In a first series of calculations the KQQM1 ON option (Simplified method for calculating momentum and heat transfer) was chosen. These results show that this version of the code cannot be used to approximate the sloshing problems. Only in the initial stages the AFDM-KQQM1-Code produces results which make sense. A typical sequence of the computational results is shown in Figure 5.1, 5.2 for Test Problem 3. The number of grid zones is 23 x 43. The plot in Figure 5.1 shows the initial values for the volume fraction of the water. Each plot shows the contour lines as well as a 3D-plot /15/. To see the surface of the water the plot was turned by an angle of 120 degrees. The plot 5.2 a) shows the water wave arriving at the cylinder wall at about time t = 0.13. Up to that stage it resembles the analytical solution by the shallow water equations as well as the experimental results. Next, the sloshing at the cylinder walls starts. The plot b.) in Figure 5.2 shows this sloshing at a time where the maximal value is reached. We observe that no grid cell contains pure water. Also at the bottom of the cylindrical container the volume fraction of the water does not exceed 88 per cent. That means the air which mixes with water does not leave the grid zones in later times. This becomes more obvious in the plot c.). Here, the water wave has been reflected at the cylinder wall and converges now in the center. The volume fraction of the water in the whole domain is not greater than about 73 per cent.

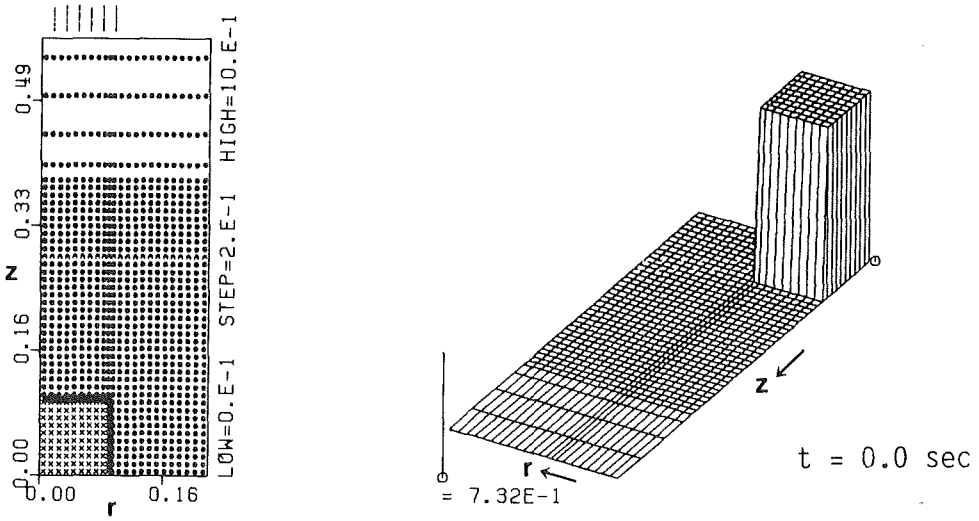


Figure 5.1: Initial values of the water volume fraction for Test Problem 3

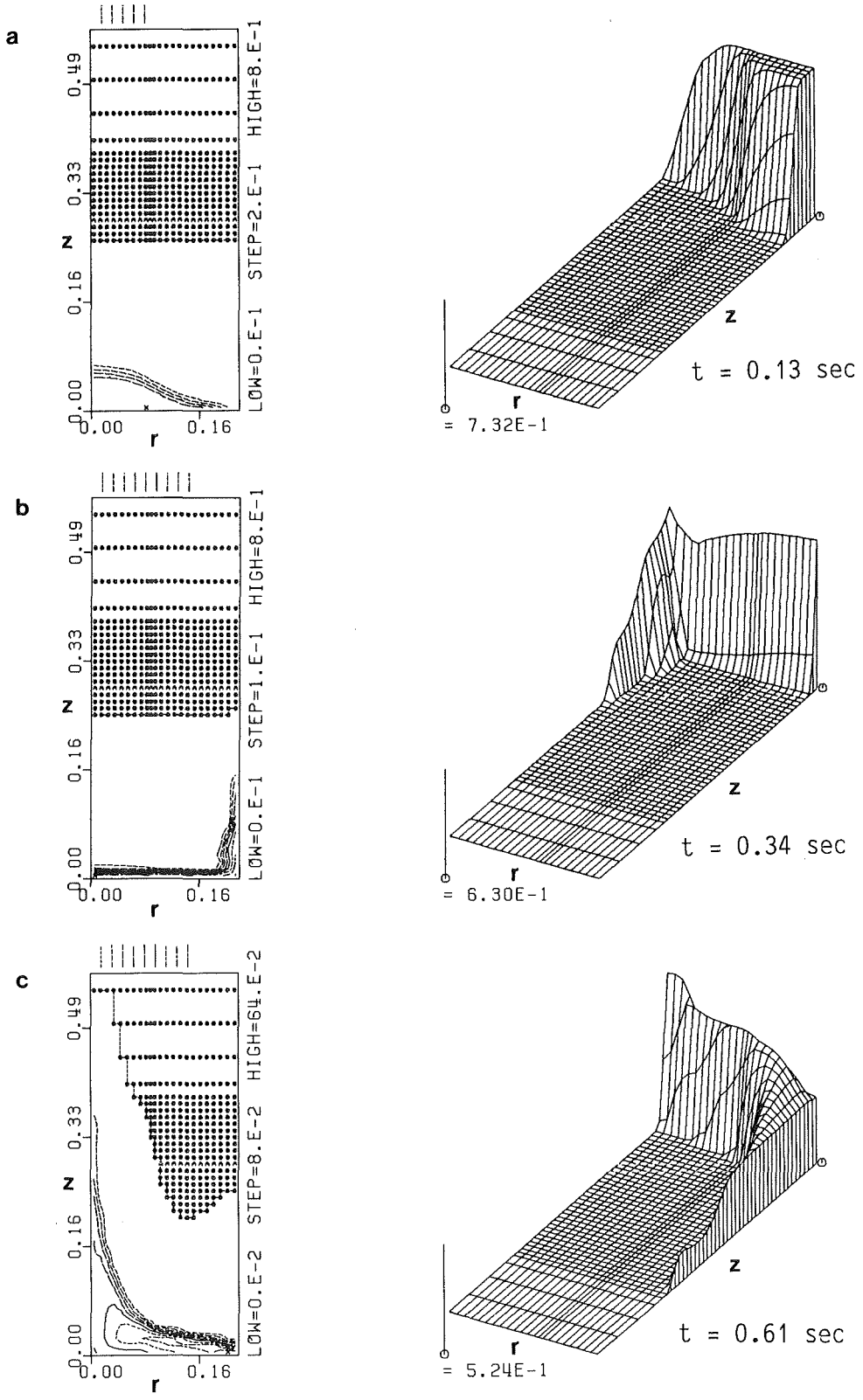


Figure 5.2: AFDM results with KQQM1 ON option for Test Problem 3 at different times

This does not agree with experimental results or theoretical considerations. The consequence of this failure is that the maximum values of the sloshing height is strongly overpredicted. Depending on the amount of water the maximum values at the cylinder wall become greater up to a factor of two, at the central collaps up to a factor of three or more compared to the experiments.

## 5.2 KQQM2-Option

In a second series of calculations KQQM2 ON and ARCV1 ON (Standard models for momentum and heat transfer) were chosen while KQQM1 was switched off. The number of grid zones is 23 x 43 and the spacing as described in Section 4. Again the results of Test Problem 3 were picked to give an impression of the process. The main stages become visible in Figure 5.3 a - f. At about time t = 0.14 the rarefaction wave reaches the outer cylinder wall and the water is pushed up. The maximum water height is 12 cm at time t = 0.4 sec. The movement of the water stops and the water falls down to the bottom generating a water wave traveling and converging towards the axis. At about t = 0.53 sec this cylindrical wave arrives at the center and sloshes up to a height of 22 cm at time t = 0.76 sec. During the whole process areas exist with pure water (volume fraction ≈ 1.0). Contrary to the results with KQQM1 ON option, the air is swept out of the grid area at the bottom when the reflected water wave is travelling to the center. At the time of the central collaps pure water at the bottom exists. This is in agreement with the experimental results.

The results for all test problems obtained by the AFDM-Code, are listed in Table 5.1. For all test problems the structure of the experimental solution is matched

| Test problem | $t_1$ [sec] | $t_2$ [sec] | max. $h_{sl}$ [cm] | $t_3$ [sec] | max. $h_{co}$ [cm] |
|---|---|---|---|---|---|
| 1 | 0.19 | 0.32 | 5 | 0.92 | 3 |
| 2 | 0.19 | 0.38 | 13 | 0.94 | 50 |
| 3 | 0.14 | 0.29 | 10 | 0.76 | 22 |
| 4 | 0.14 | 0.34 | 20 | 0.80 | 55 |
| 5 | - | 0.36 | 12 | 1.22 | 24 |

Table 5.1: Results of the AFDM-Code for the Test Problems, 23 x 43 grid zones

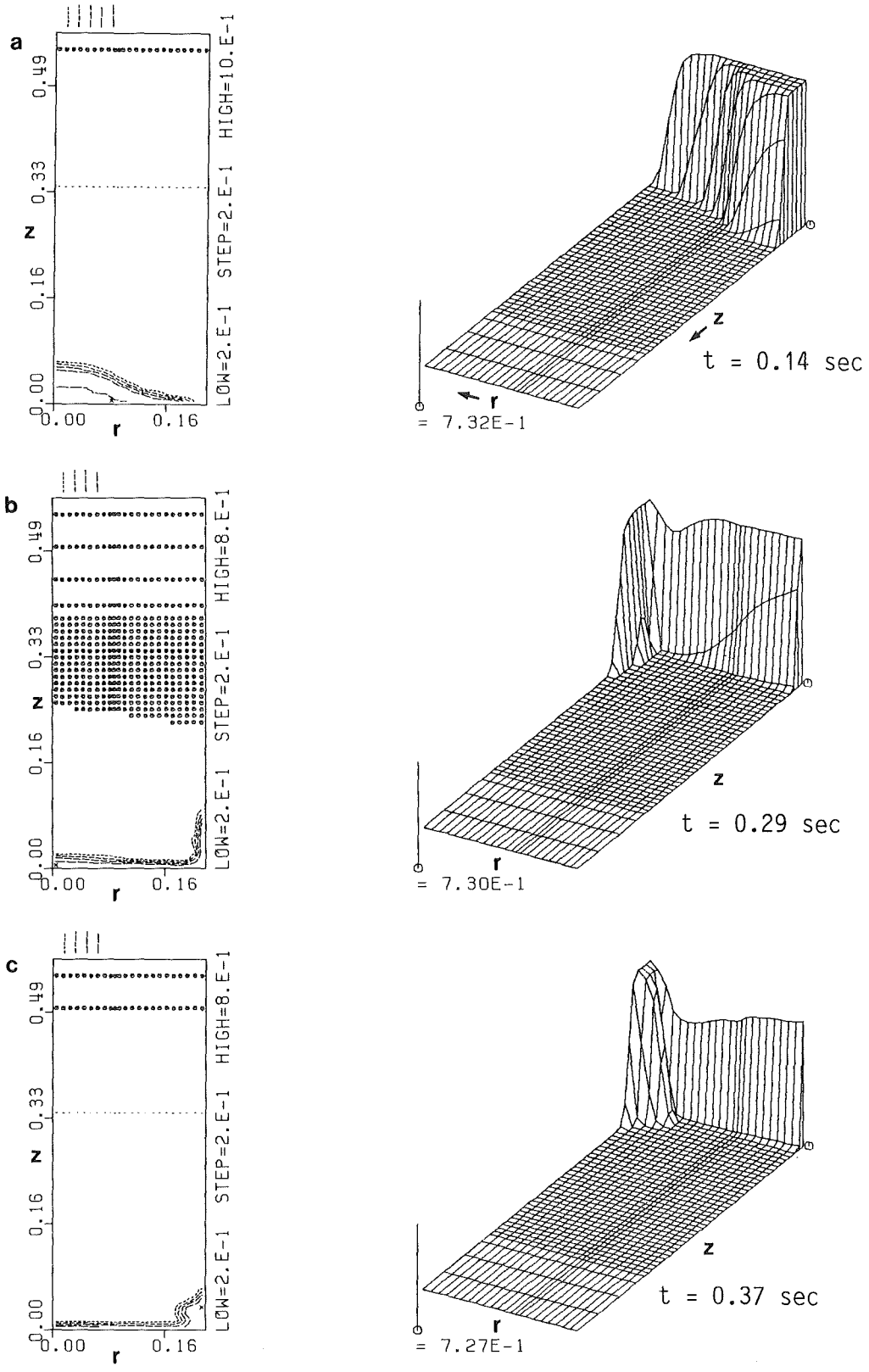


Figure 5.3: AFDM-Code results with KQQM2 ON option for Test Problem 3 at different times

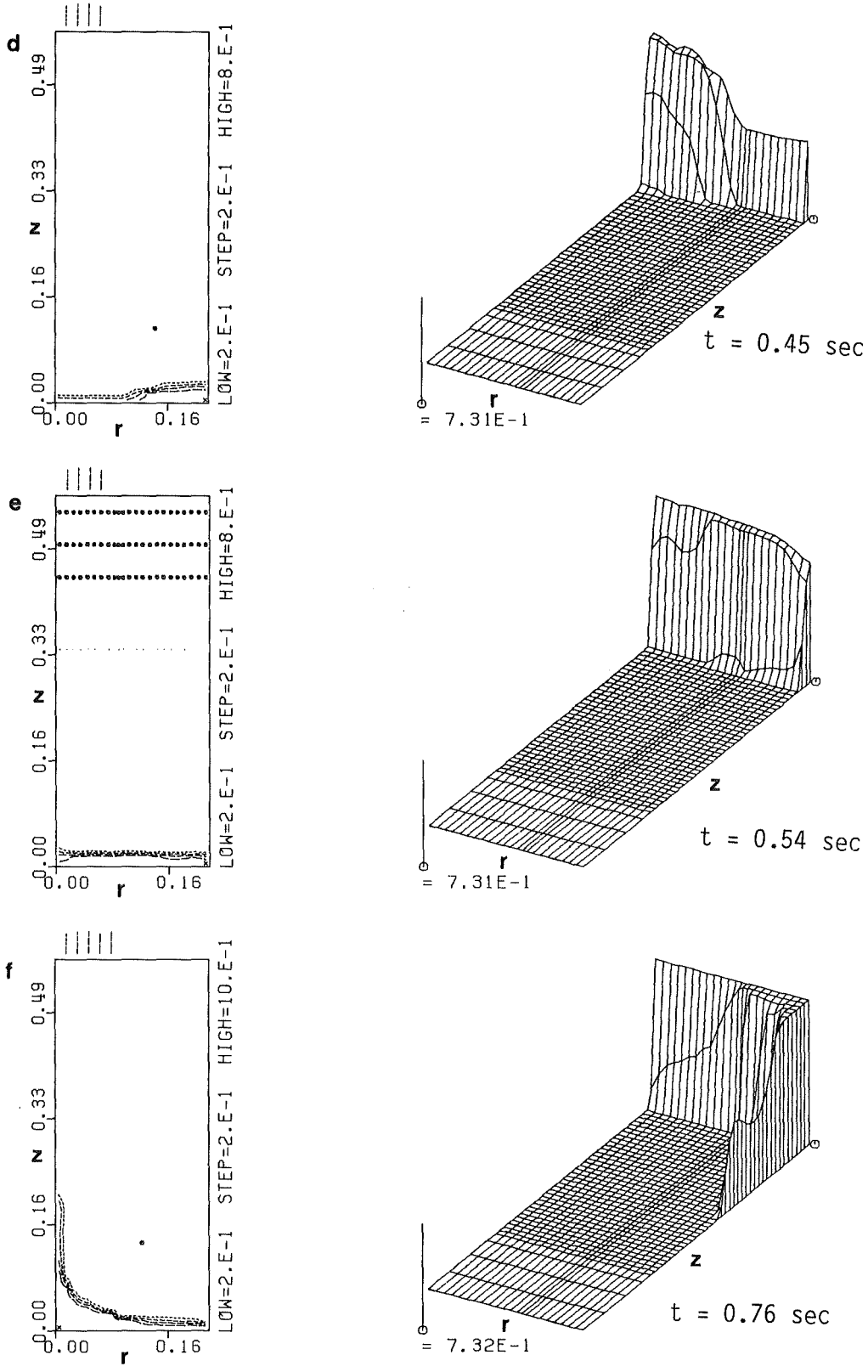


Figure 5.3: continued

well. The different times measured in the experiments and determined in the numerical results agree within a range of about 10 per cent. It is observed that the times for arrival and first sloshing are always smaller in the numerical results. This may be due to two different facts. The numerical dissipation introduces some type of smearing of the wave fronts, which will e.g. cause that the water arrives at the outer cylinder a little bit earlier. This fact is supported by the results of a third series of calculations on a finer grid, presented below. Here, the times tend to a little bit higher values. Another possibility may be the friction at the bottom and the wall which is not taken into account in the numerical calculations and which may increase the time durations in experiments. The results for the maximal sloshing heights at the outer cylinder wall show that in the first and second Test Problem the height is clearly underestimated by the numerics, while in the other problems they compare better. The main difference between Test Problem 1, 2 and the others is that we have a smaller volume of water in the container. We observe that during the calculation the volume fraction of water in the grid zones at the bottom will decrease below 50 %. The interpretation of this situation as bubbly or pool flow, as done in the AFDM-Code, will lead to inaccurate results in the dynamics. This inaccuracy should increase by further reducing the volume of water inside the container and should decrease by grid refinement. Both facts were observed in the calculations.

While in the dam break problems the qualitative structure of the numerical solution is quite similar to the shallow water equations solution (see Figure 3.1), in the water step problem no constant state behind the water wave to the right (see Figure 5.4) is obtained. This phenomenon is also clearly visible in the experimental results (see Figure 2.6). This is mainly an effect of the large water depth so that the shallow water approximation is not valid, and also an effect of geometry. Calculations of this water step problem were performed with the step a long distance away from the axis to obtain results which are quite similar to the plane case without effects of geometry. It was observed that also in this case no constant state exists behind the water wave to the right. The profile behind the front of the wave decreases monotonously up to the rarefaction wave traveling to the left. The main difference between the cylindrical and plane problem is that the minimum is much smaller in the first case. The geometry accentuates that structure, decreases the minimum and flattens the wave. But the form of the wave is due to the influence of the "deep" water, which can not be obtained by the shallow water solution. We have pressure waves inside the water which lead to fluid flow and a balancing of the water tides. The inner water height decreases and the

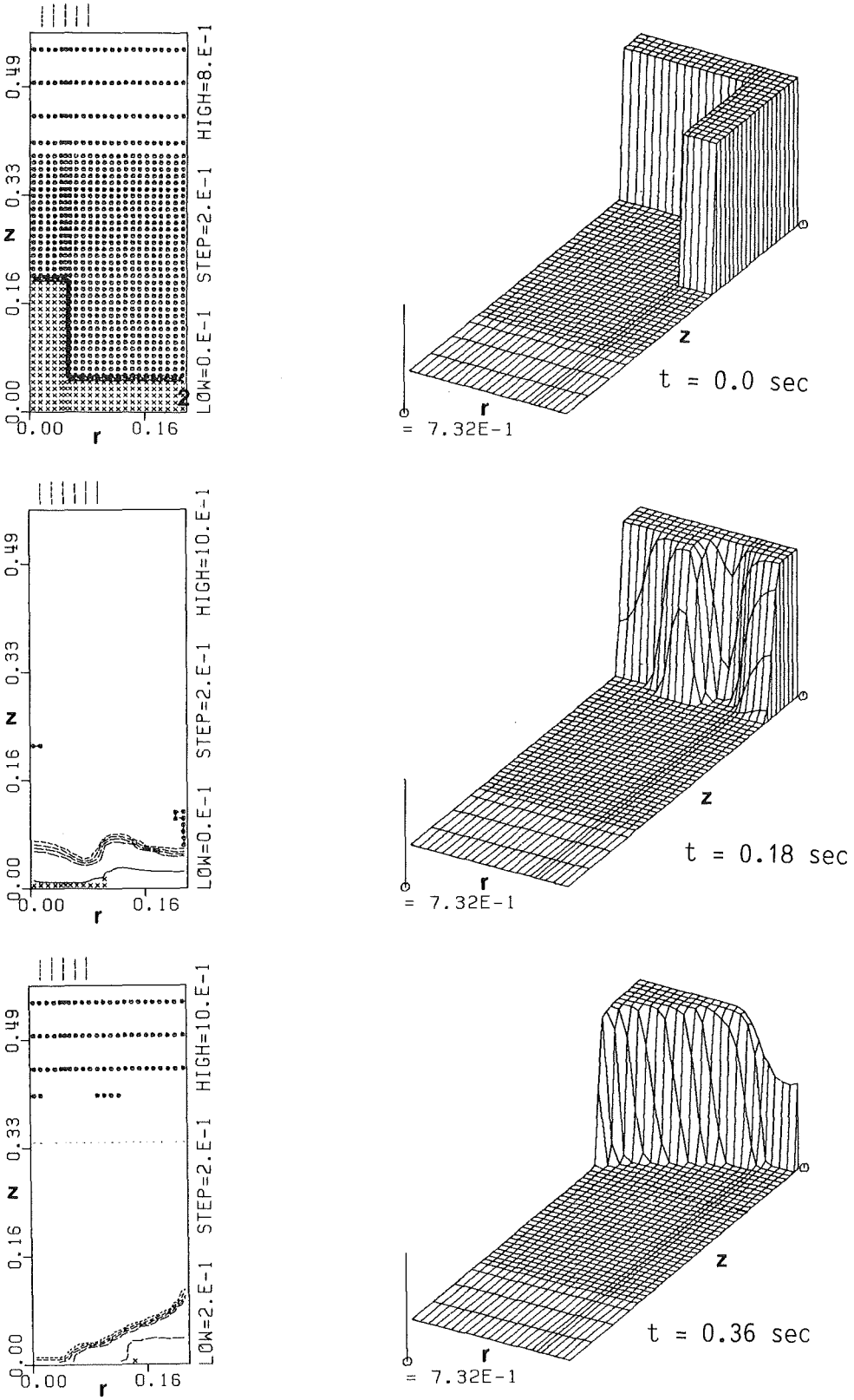


Figure 5.4: AFDM-Code results with KQQM2 ON option for Test Problem 5 at different times

outer increases. The time scale of the pressure waves is given by the sound velocity of water. In Figure 5.4 one can see that at time t = 0.18 the inner and outer water column have nearly reached the same height. The time scale of the surface waves is given by velocity $c_o = \sqrt{gh}$ = 1.4 m/sec (see Figure 3.1) which is much smaller than the sound velocity in water. Hence, the fluid flow of the water initiated by the pressure waves will play a significant role. It can be seen that the decrease of the height of the whole inner water column starts in the very beginning before the rarefaction wave reaches the center.

In the experimental data for Test Problem 5 at about t = 0.64 a first sloshing at the center was observed. But this was only a first small hump with a large base but with a height of only 20 cm. This first sloshing follows a very narrow and high collapse with height of above 50 cm at time t = 1.24 sec. This main sloshing height is listed in Table 2.2. In the numerical results of the AFDM-Code we see a similar behaviour, but the first slosh is higher (h = 28 cm) and the second slosh is smaller (h = 24 cm). The sloshing times are quite similar (t = 0.36 sec, t = 1.22 sec, respectively). For larger times several smaller sloshes appear in experiment as well as in the numerical results in a periodical manner.

In a third series of calculations we refined the grid up to 46 x 86 grid zones. The results are summarized in Table 5.2.

| Test problem | $t_1$ [sec] | $t_2$ [sec] | max. $h_{sl}$ [cm] | $t_3$ [sec] | max. $h_{co}$ [cm] |
|---|---|---|---|---|---|
| 1 | 0.19 | 0.33 | 8.5 | 0.85 | 24 |
| 2 | 0.19 | 0.39 | 16.0 | 0.94 | 60 |
| 3 | 0.14 | 0.30 | 13.0 | 0.78 | 55 |
| 4 | 0.14 | 0.38 | 25.0 | 0.88 | 55 |

Table 5.2: Results of the AFDM-Code for the Test Problems, fine grid

They confirm the results on the coarse grid. The sloshing heights at the outer cylinder wall become greater. They agree for Test Problem 1 - 3 very well with the experimental results. The defect of the results on the coarse grid for Test Problem 1 vanishes. For Test Problem 3 and 4 the sloshing heights are a little bit over-estimated in comparison with the experimental results. This may be due to the perfect radial symmetry imposed in the numerical calculations which cannot be obtained in the experiments. Another reason may be that our calculations are

without viscosity. On the coarse grid the numerical method introduces numerical dissipation which is larger than the physical one. On fine grids the numerical dissipation may be reduced up to a level such that the real physical viscous terms are greater. Because the AFDM-Code has no possibility to switch on viscous terms, this topic cannot be studied. (In SIMMER viscous terms can be added optionally for the solution but the first order method has such a high "artificial viscosity" that no discrimination is possible between both options.) The calculations on the fine grid reveal much more details than on the coarse grid. As an example in Figure 5.5 the results on the coarse and fine grid for Test Problem 2 are shown when the maximum sloshing height is reached. The numerical solution on the fine grid agrees with our experimental observations very well.

Optionally AFDM can be run using donor cell differencing. This first order method is known to introduce considerable artificial damping in the solution. Some calculations for comparison were made with the second order solution as well as with the results of SIMMER-II which uses a similar numerical method (see Section 7). In Figure 5.6 results of Test Problem 3 are displayed where the maximal sloshing heights at the outer wall and in the center become visible. The comparison with the second order results in Figure 5.3 shows that the sloshing heights are strongly reduced: from 10 cm to 8 cm at the outer wall and from 22 cm to 11 cm at the center. The results are summarized in Table 5.3.

| Test problem | $t_1$ [sec] | $t_2$ [sec] | max. $h_{gl}$ [cm] | $t_3$ [sec] | max. $h_{co}$ [cm] |
|---|---|---|---|---|---|
| 3 | 0.13 | 0.27 | 8.0 | 0.69 | 11 |

Table 5.3: Results of the AFDM-Code for Test Problem 3 (23 x 46 grid zones) using donor cell differencing option

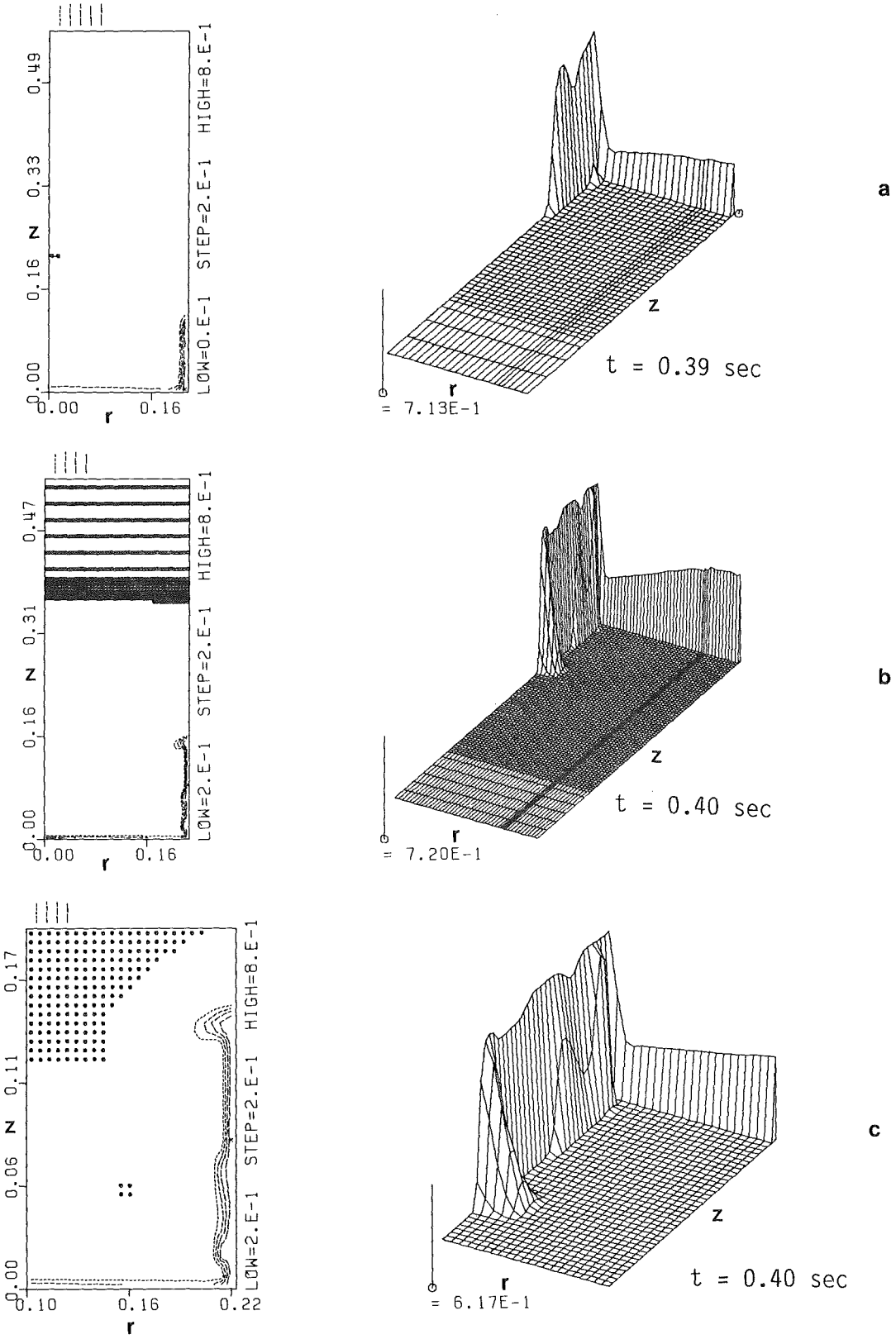


Figure 5.5: AFDM-Code results for Test Problem 2 on a.) coarse b.) on fine grid; c.) shows b. in detail

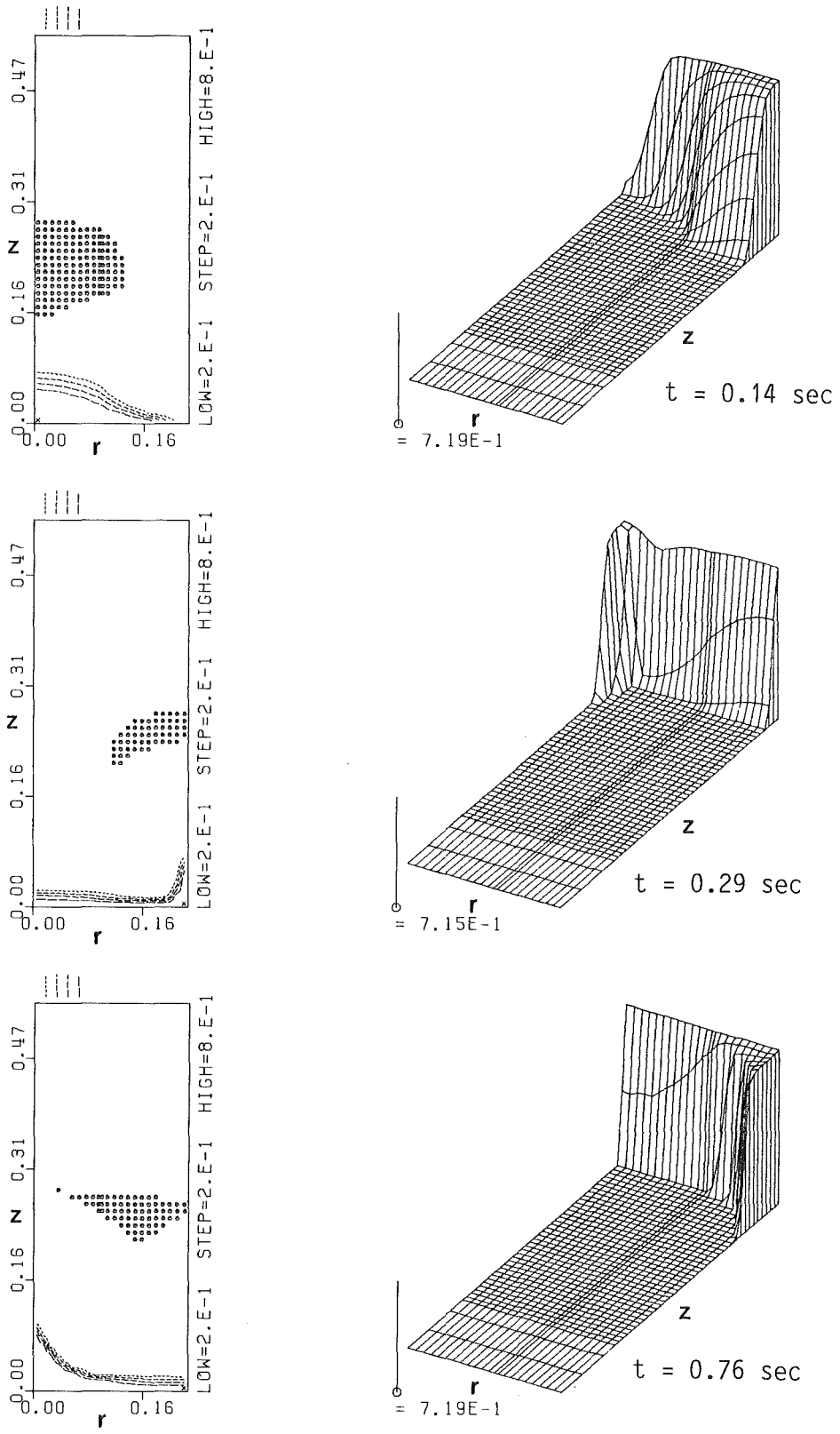


Figure 5.6: AFDM results for Test Problem 3 using the donor cell differencing option

## 6. Time step Sensitivity

In many problems of the AFDM-Assessment especially those for problems including heat and mass transfer phenomena time step sensitivities have been observed. If the physical problem is well-posed, this behavior must be introduced by mathematical or numerical modelling or coding errors which means that the approximation is not consistent with the physical problem. For the sloshing problems considered here it is known that these problems are well-posed in the first stages up to the time when the collaps will start. Only close to the collaps the real three-dimensional problem becomes unstable, which cannot be reproduced by a two-dimensional code, where symmetry is imposed. Hence the sloshing problems seem to be good candidates for studying the time step sensitivity of the AFDM-Code. We note that these problems will give insight into the AFDM hydrodynamic part only. The sloshing problems do not give any information about the behavior of the numerical heat and mass transfer modelling.

Calculations were performed with several values for the Courant number. A Courant number COURTN = 0.2 has been used for all results, presented above. The results obtained with Courant numbers 0.4, 0.2, 0.04 and 0.02 were compared and only slight differences were found. As an example the results for Test Problem 3 with Courant number 0.04 are chosen. These results are shown in Figure 6.1. A comparison with the plots of Figure 5.3 shows that almost identical results are obtained.

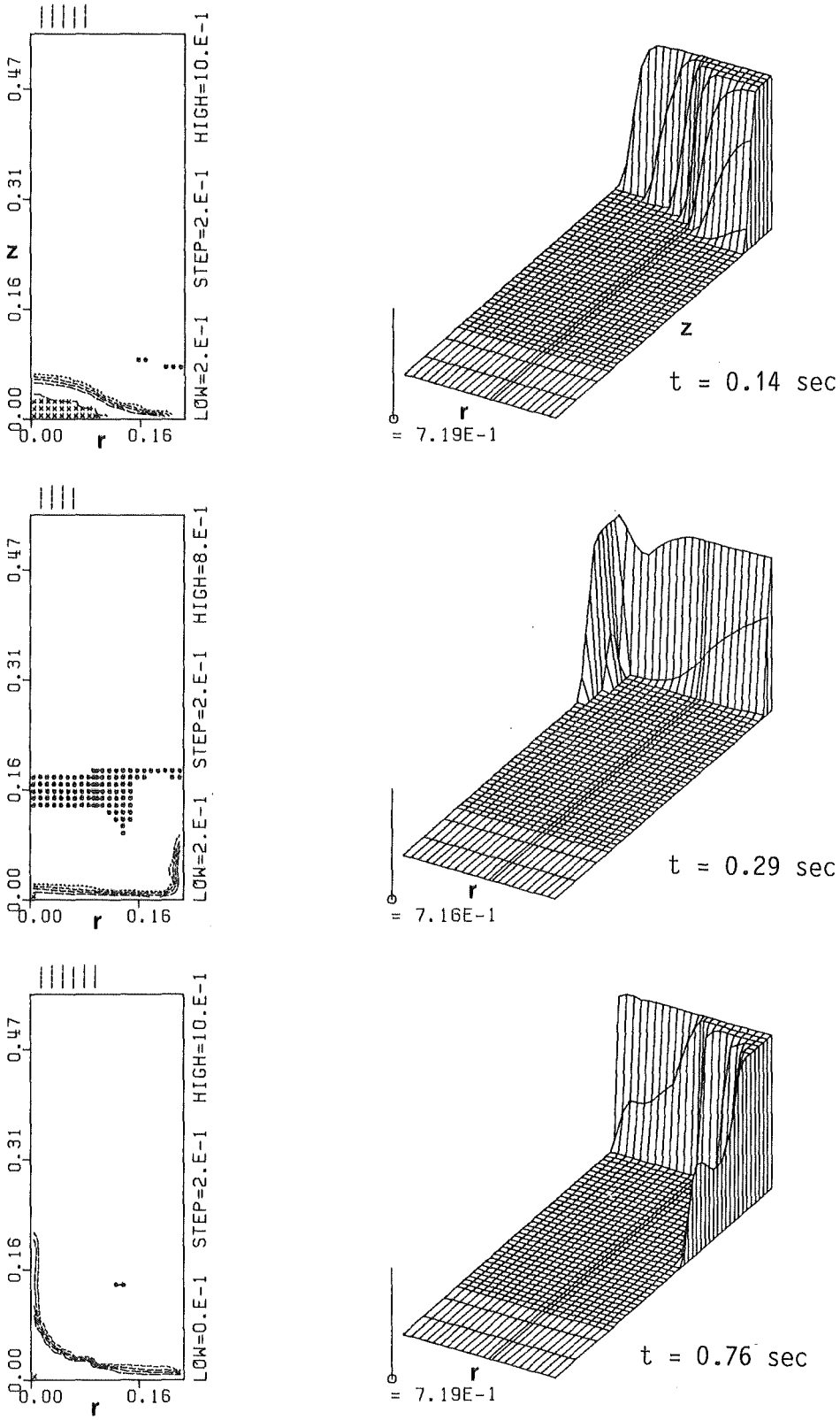


Figure 6.1: AFDM-Code results for Test Problem 3 with Courant number 0.04

## 7. SIMMER-II Results

The SIMMER code uses first order donor cell differencing with its known numerical damping, rising the question if this method is adequate to describe sloshing motions correctly. As also the AFDM code can be run using donor cell differencing the results from both codes could be compared directly and also deviations from the second order method could be made visible. In Fig. 7.1 the corresponding motion patterns to Fig. 5.3 are given.

It is clearly visible from the comparison of this figures that both donor cell methods in SIMMER and AFDM give similar results. Compared to the second order method (which is rather close to the experiment) the known numerical viscosity of donor cell differencing leads to an underestimation of sloshing heights at the outer cylindrical wall and during the collapse phase in the center (see Tab. 7.1).

| Test problem | $t_1$ [sec] | $t_2$ [sec] | max. $h_{gl}$ [cm] | $t_3$ [sec] | max. $h_{co}$ [cm] |
|---|---|---|---|---|---|
| 3 | 0.12 | 0.27 | 8.0 | 0.72 | 13.0 |

Table 7.1: Results of the SIMMER code for the Test Problem 3 (23 x 43 grid zones)

Compared to the AFDM solution (and experiment) all times are smaller which should be an effect of the numerical diffusion spreading the wave fronts over several grid zones. This tendency is also obvious in the results for the other test problems.

Similar as for the AFDM calculations the time step sensitivity was tested for Problem 3 reducing the Courant number from originally 0.2 to 0.04.

As can be seen from Fig. 7.2 SIMMER results show a small influence of the chosen time step on the local shape of the water waves in the low liquid regions. Both the water peaks of the out-slosh and in-slosh configurations are nearly identical for both Courant numbers.

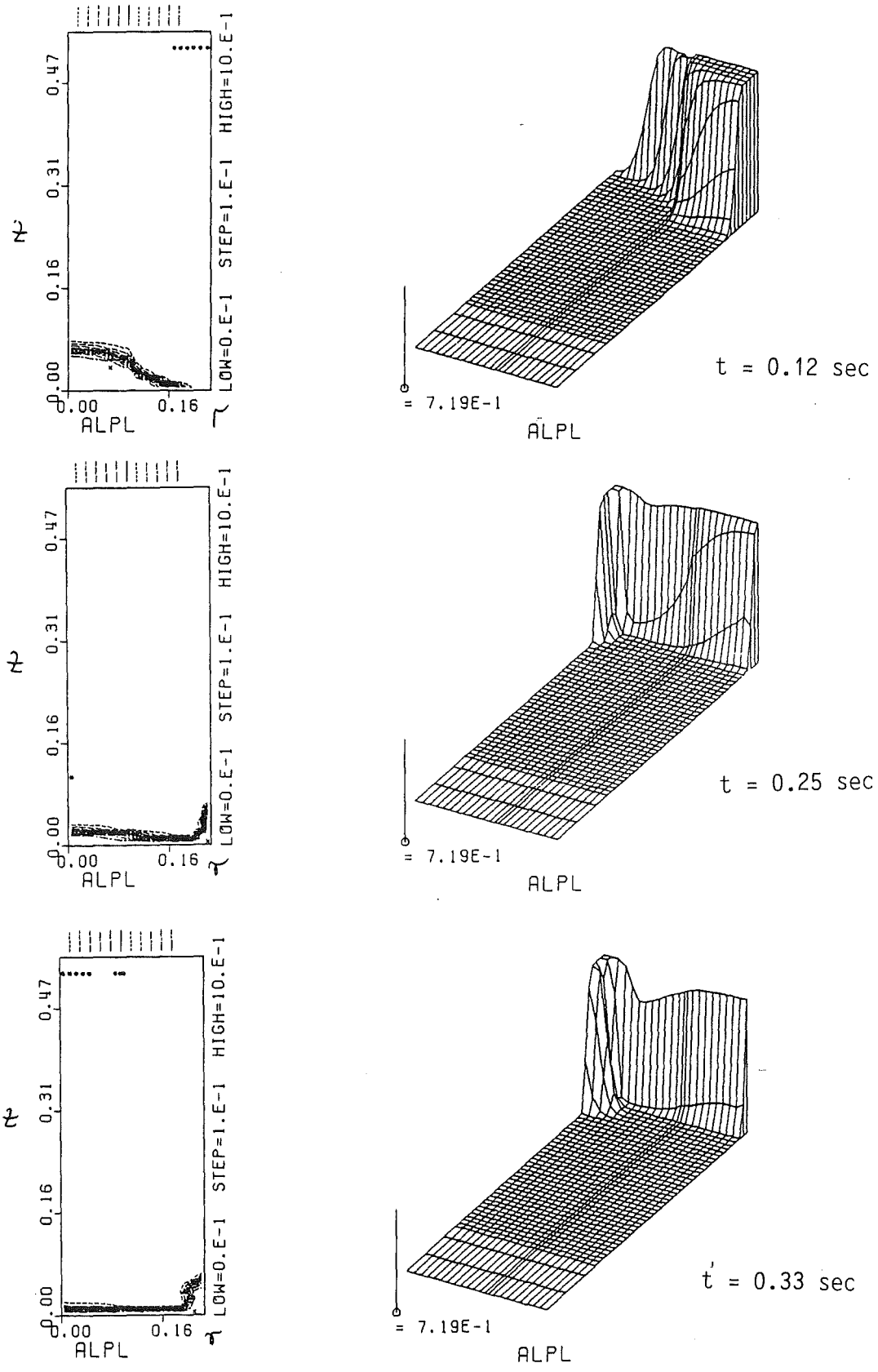


Figure 7.1: SIMMER results for the Test Problem 3 at different times

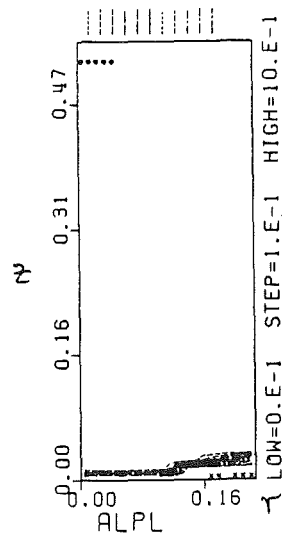


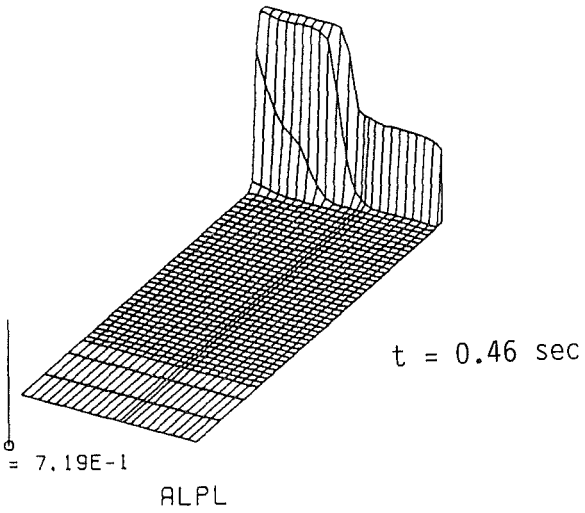


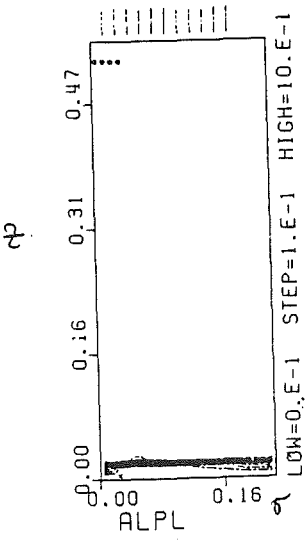


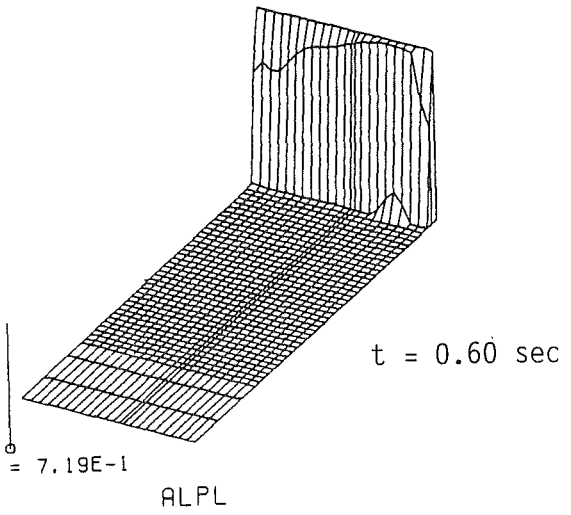


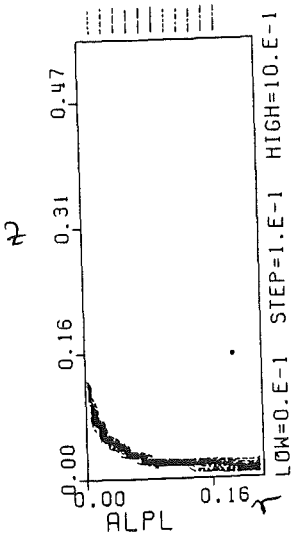


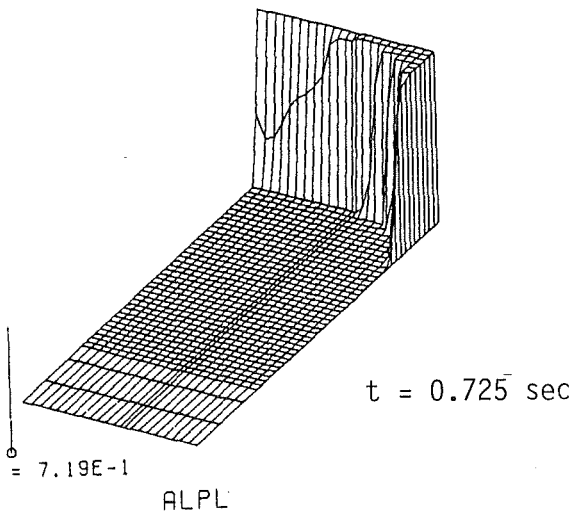


Figure 7.1: continued

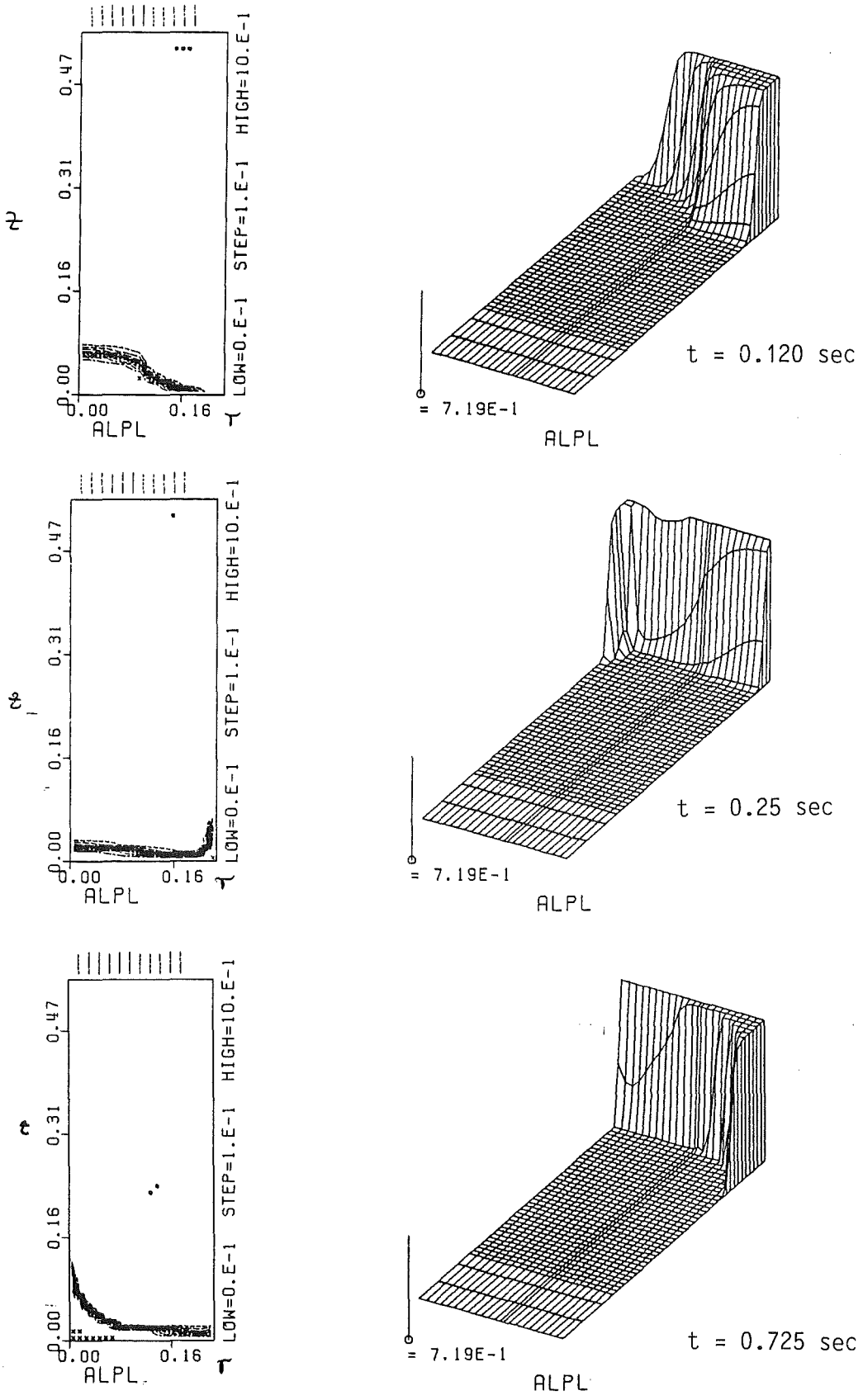


Figure 7.2: SIMMER-Code results for Test Problem 3 with Courant number 0.04

## 8. Sloshing Simulation with Obstacles in the Flow

To increase the complexity in the code simulation of the sloshing processes obstacles were placed into the flow. Plexiglas rings of different heights were placed on the bottom of the large container between the central water column and the outer container wall.

The conditions and results of a typical experiment with a 2 cm and a 3-cm-high obstacle are given in Table 8.1. The experimental results are displayed in Fig. 8.1 and Fig. 8.2. Because we have symmetric cylindrical conditions, the fluid motion could be simulated with the AFDM and the SIMMER-II codes.

Figure 8.3 displays some selected results of volume fraction plots of both calculations SIMMER-II and AFDM. To capture all the details of fluid motion as seen in the experiment, a finer mesh grid ($\Delta r/2$, $\Delta z/2$) had to be used for the code calculations. As can be seen in Fig. 8.4 and Fig. 8.5, the experimental behavior of fluid motion of the outward slosh is then adequately reproduced by AFDM. As can be seen from the comparison of both experiments with different step heights the outward moving wave front of experiment 7 touches the outer wall at a level of $\sim$ 20 cm whereas in experiment 6 the fluid wave contacts the wall only near the bottom of the container. This behaviour is perfectly simulated in the AFDM calculations.

Note that both the AFDM and the SIMMER calculations overestimated the central sloshing heights in the case of an obstacle at the lower pool boundary. While the flow disturbances in redirecting fluid motion are so strong that a central slosh can hardly develop in the experiments, both codes (not simulating the azimuthal instabilities) underestimate the effect of the obstacle. The central sloshing heights in SIMMER are higher than those in AFDM because with AFDM less liquid is transported across the obstacle during the outward slosh. The central sloshing results from the water left within the plexiglas ring. The experiments and the calculations demonstrate that the central sloshing heights are drastically reduced when there is an obstacle in the flow compared with the sloshing heights of the unimpeded flow.

| | $H_{column}$ (cm) | $H_{obstacle}$ (cm) | $H_{water}$ in Container (cm) | Experiment: Central Sloshing Height [cm] | AFDM Central Sloshing Height (AFD2) [cm] | SIMMER Central Sloshing Height (SIM) [cm] |
|---|---|---|---|---|---|---|
| Experiment 6: dam break | 20 | 3 | 0 | 5.0 ± 3 | 10.0 | 13.0 |

Table 8.1: Influence of Obstancles at the Pool Bottom

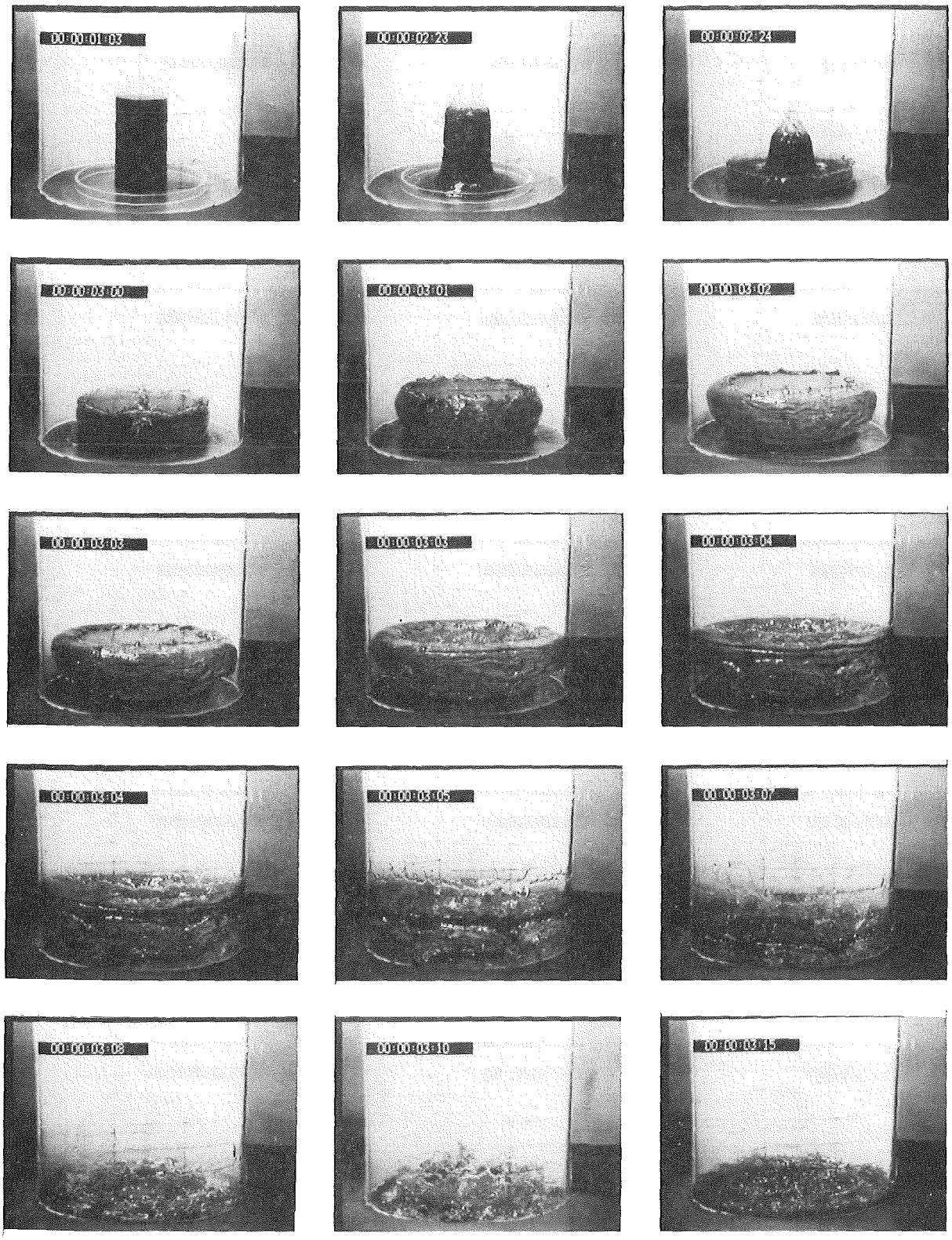

Figure 8.1: Sloshing behavior in the presence of obstacles at the pool boundaries: experimental results (2 cm obstacle)

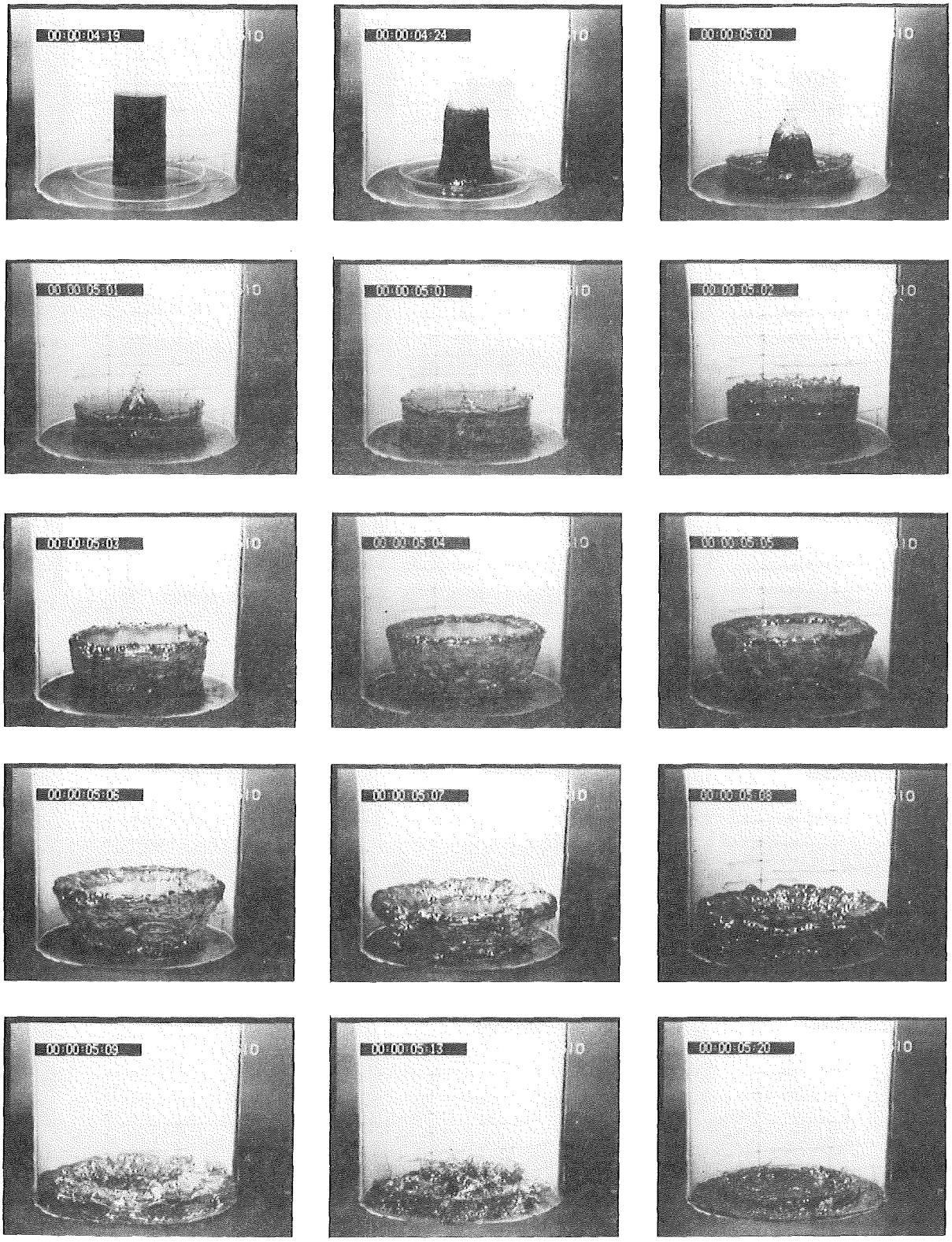


Figure 8.2: Sloshing behavior in the presence of obstacles at the pool boundaries: experimental results (3 cm obstacle)

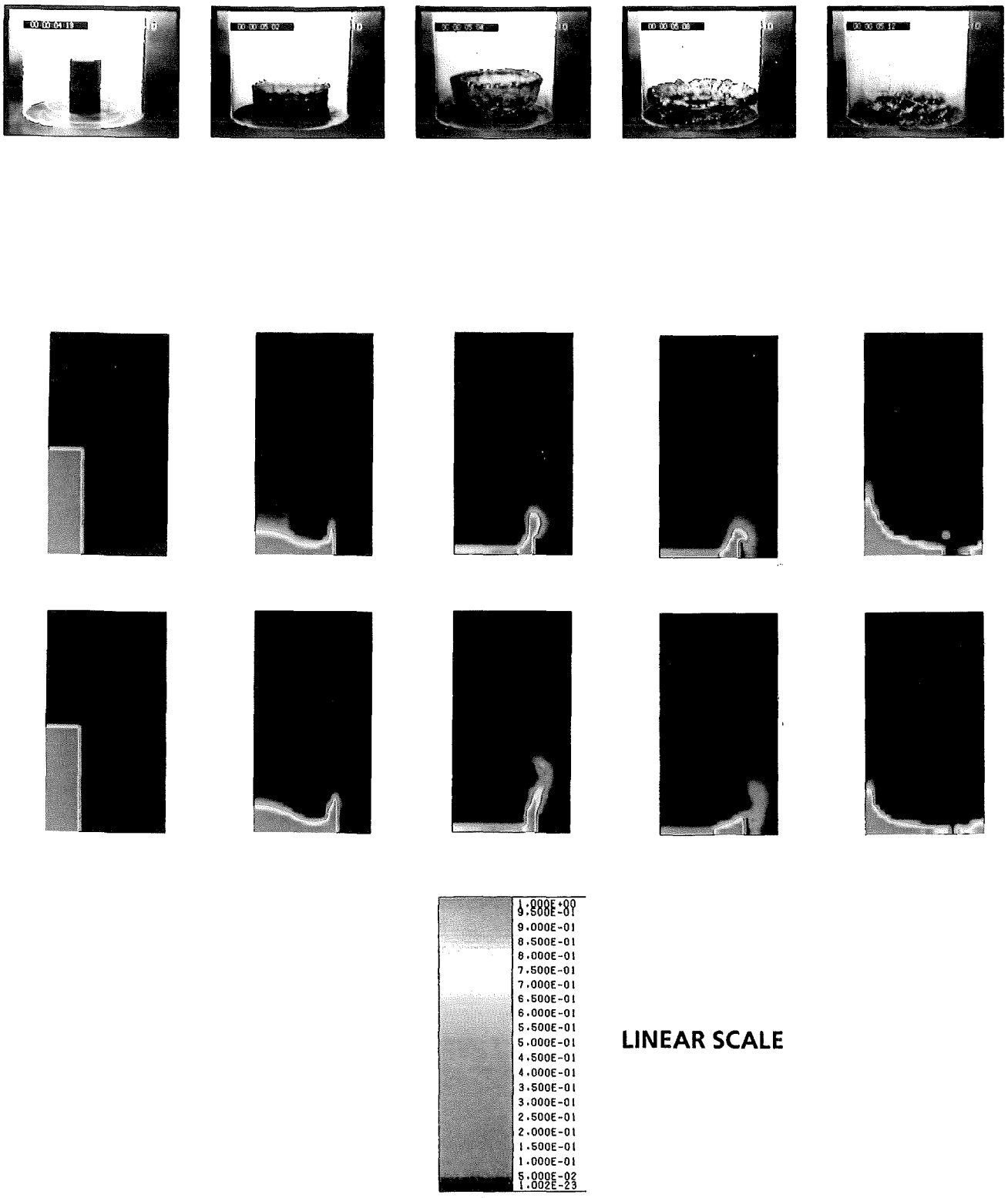


Figure 8.3: Code comparison for sloshing in the presence of a 2 cm high obstacles at the pool boundary [SIMMER versus AFDM (AFD2)]: volume fraction plot (The scale is identical in all colored plots)

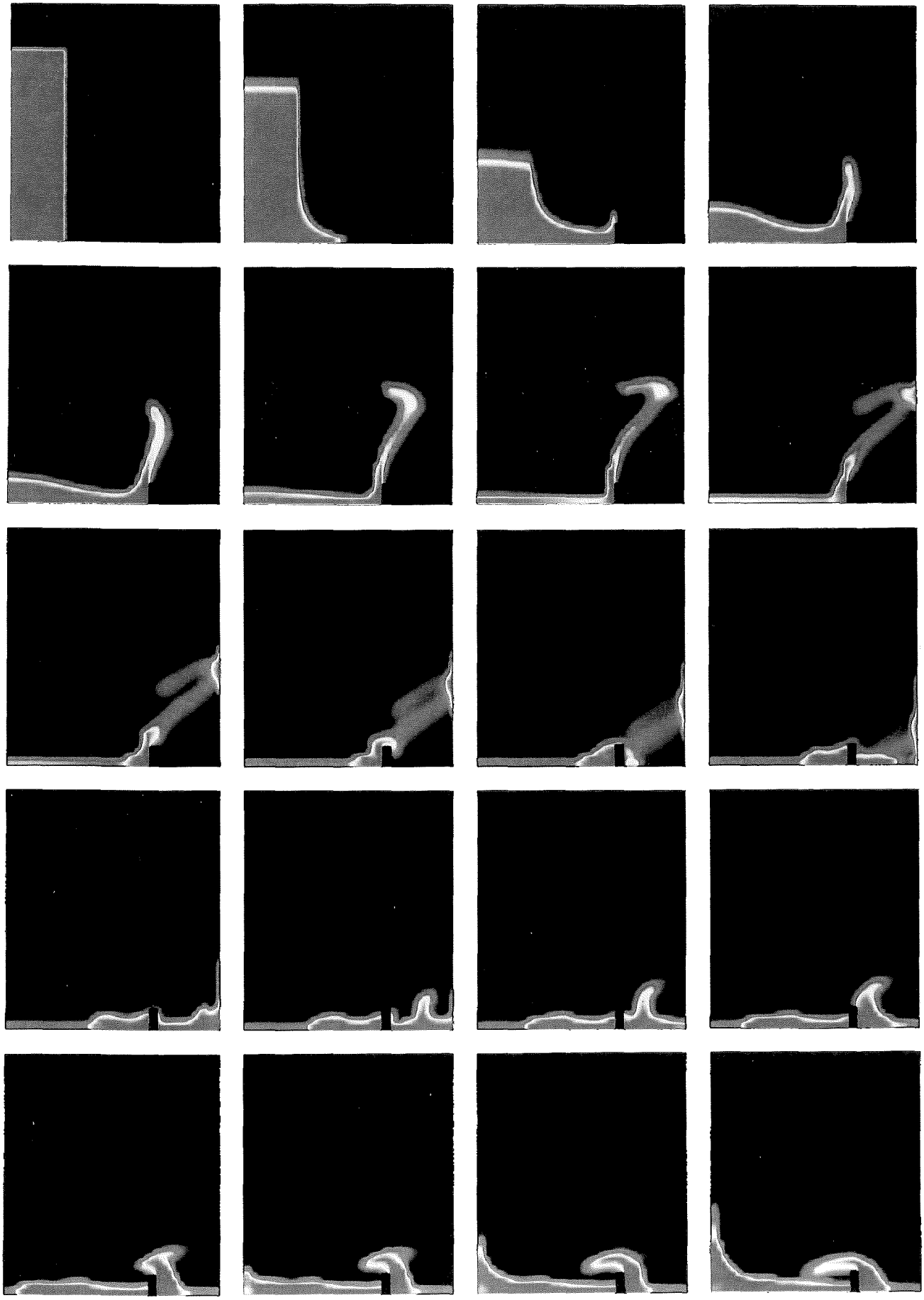

Figure 8.4: AFDM simulation with a fine mesh of a 2 cm high obstacle at the pool bottom

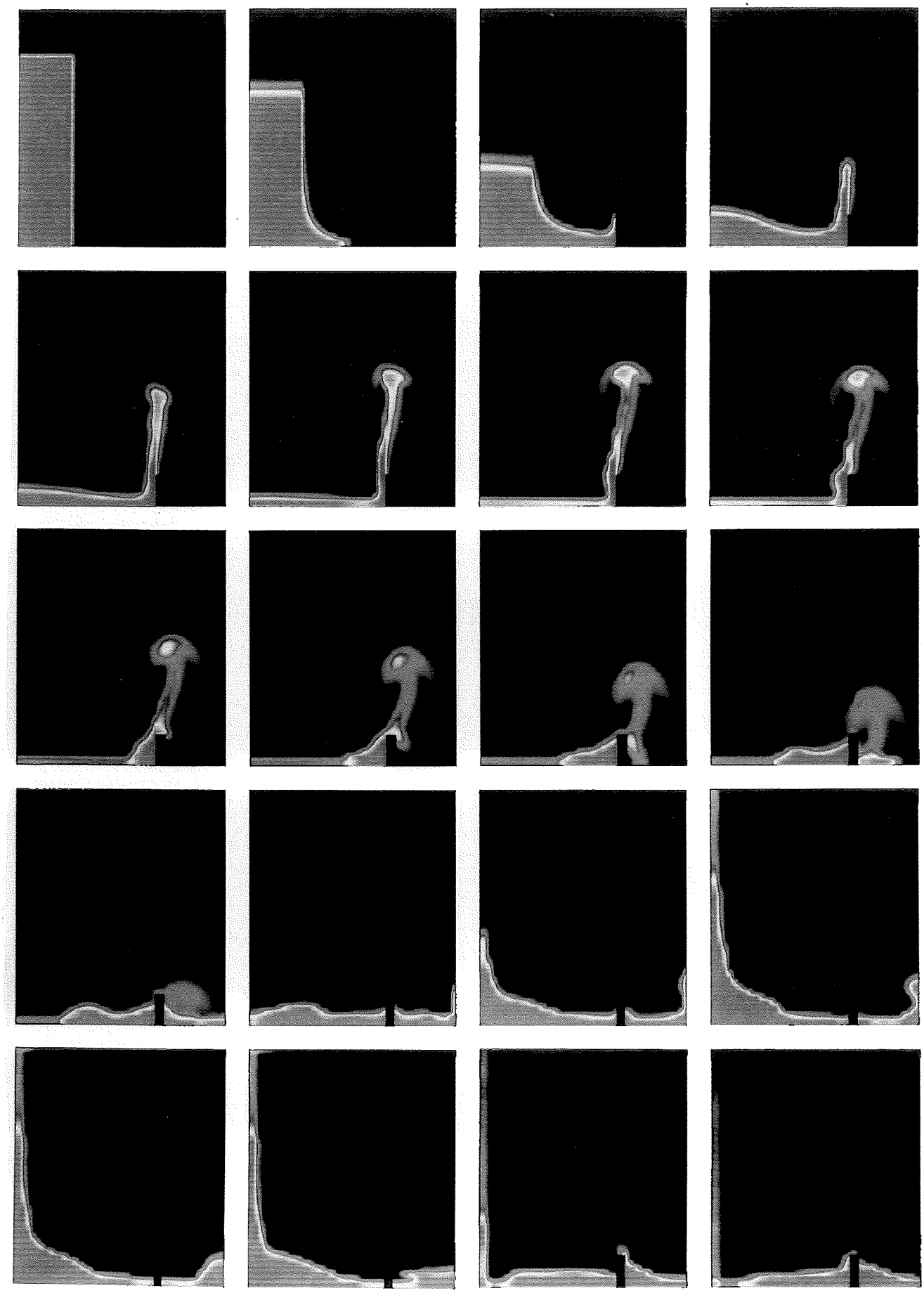

Figure 8.5: AFDM simulation with a fine mesh of a 3 cm high obstacle at the pool bottom

## 9. IVA3 Results

The IVA3-Code of Kolev /12 - 14/ uses first order donor cell differencing similar to the SIMMER II Code. It is based on the conservation equations of mass, momentum and entropy, i.e. the conservation of energy is replaced by the conservation of entropy. This is, of course, only valid as long as no shock waves in the gas phase occur. The advantage is that the equation become simpler.

The water volume fraction for Test Problem 2, predicted by IVA3, is given in Figure 9.1 as a function of the radius and the height for different times. To get a good comparison with the AFDM second-order scheme we included in this Figure the AFDM results at quite similar times and plotted all results with the same plot program. The dashed regions are predicted to be occupied by water. Furthermore we tried to include the development of the water surface as given by the experiments. The line entered on the picture is the experimentally observed surface of water. The information about it was extracted from the pictures of the high speed film camera by hand and, hence, is not very accurate, but should give a good impression of the real flow.

For the part of the experiment from the beginning to that moment when the water reaches the external boundary the results show good agreement between IVA3 and AFDM prediction and experiments. The IVA3 results show a stronger smearing of the physical discontinuities which is due to the first order differencing.

The next part of the experiment is associated with growing of the surface instability and turbilization of the mixture. Note that the form of the observed structure in Figure 2.5, shows several wiggles (usually 16 - 18 equally distributed). Obviously, these three dimensional effects cannot be predicted by a code within (r, z) format. In addition, no two-dimensional turbulence model is included in both codes. Within the numerical solution, the reflection from the wall to the center happens faster than observed in the experiment.

From the comparison of the arrival times of the water waves and their sloshing heights it becomes also visible that IVA3 produces similar results as SIMMER-II or AFDM with first order differencing. The inherent numerical viscosity leads to an underestimation of sloshing heights and to a smearing out of wave packages.

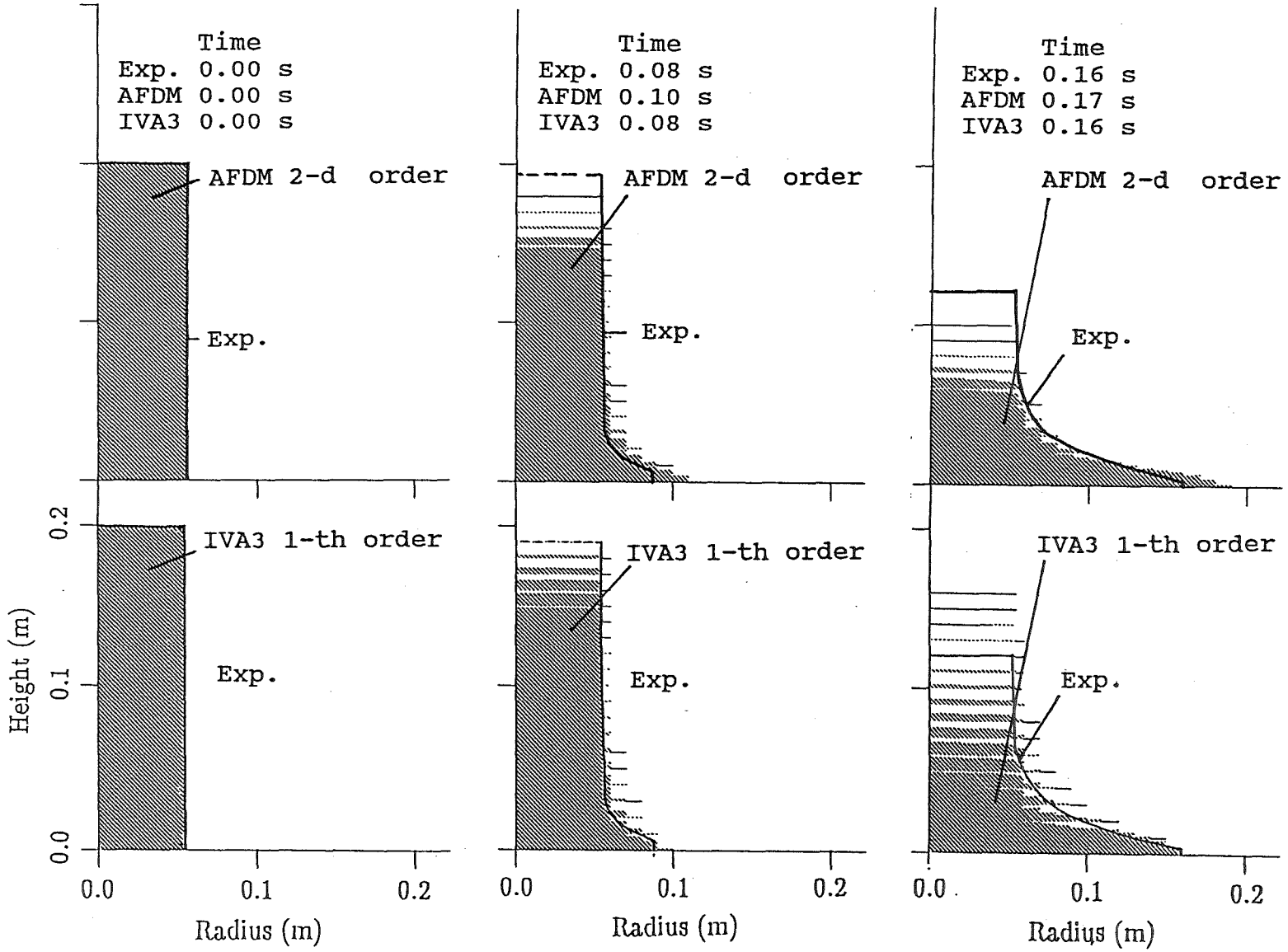


Figure 9.1a: Comparison of AFDM and IVA3 volume fraction plots with experimental data

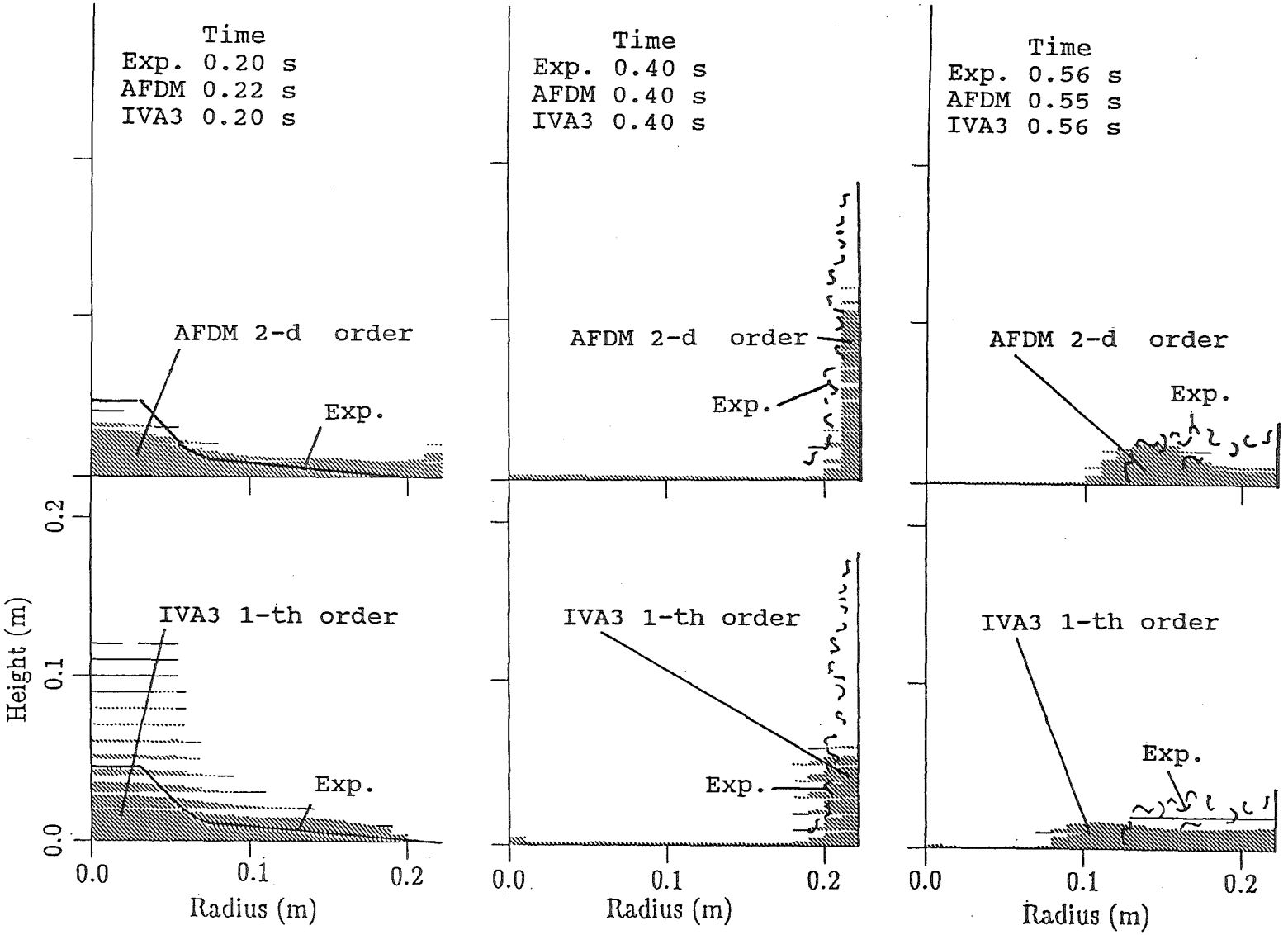


Figure 9.1b: Comparison of AFDM and IVA3 volume fraction plots with experimental data

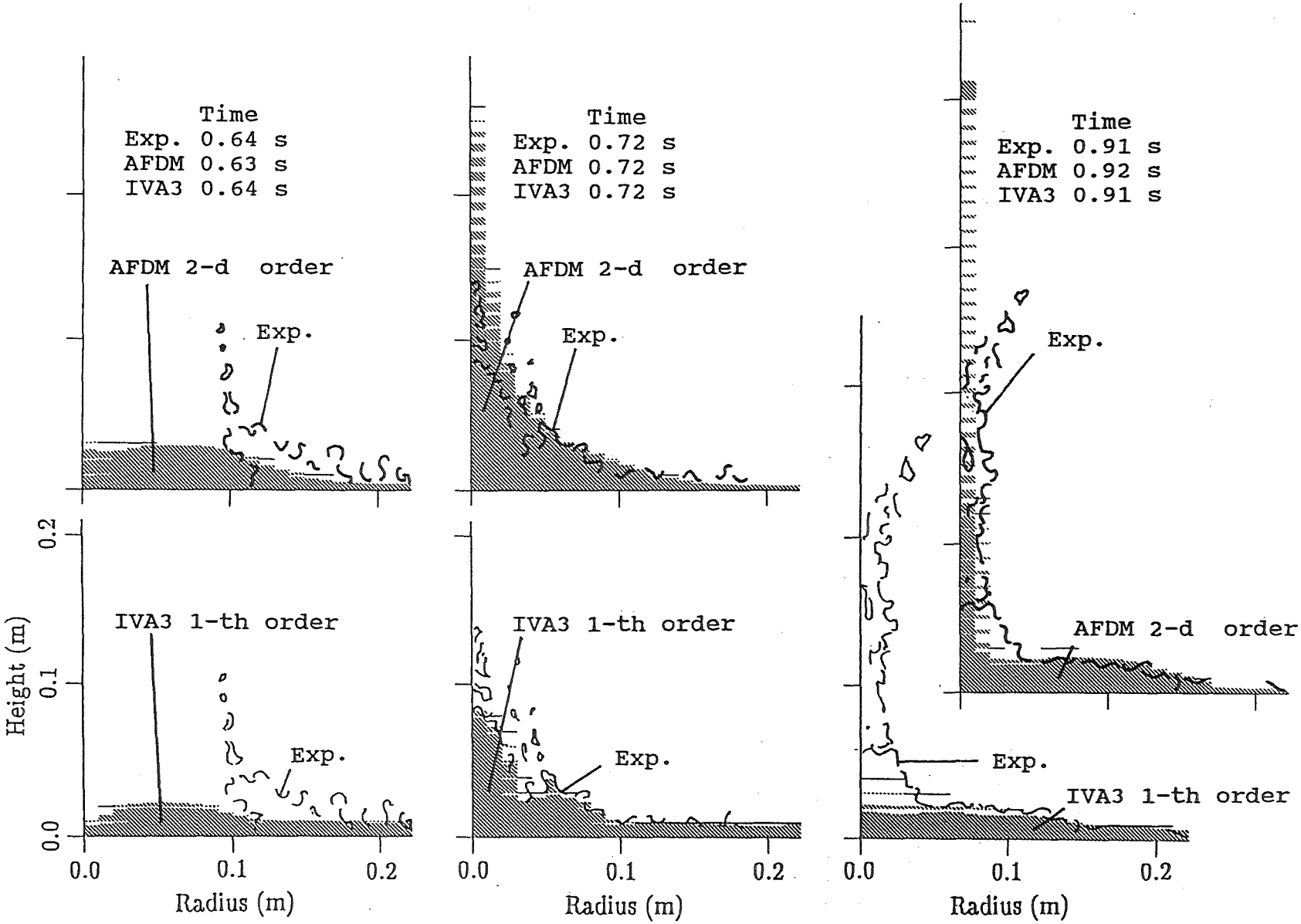


Figure 9.1c: Comparison of AFDM and IVA3 volume fraction plots with experimental data

## 10. Discussion of Results and Conclusions

Three different accident codes which describe two phase flow phenomena during accident simulation, SIMMER-II, AFDM and IVA3 have been tested in their capability to calculate sloshing fluid flow. Special experiments on "centralized sloshing" which were performed at KfK served as basis for this comparison. The experiments are clear and simple both in experimental as well as in numerical structure and are good tests to benchmark a hydrodynamic code. Both sharp fluid peaks and smooth but compact wave packages occur during the sloshing process and should be simulated accurately.

From the numerical simulation of the centralized sloshing the following conclusions can be drawn:

1) If first-order methods are applied as in SIMMER-II and IVA3, and optionally in AFDM the sloshing heights are underestimated while the sloshing velocities of the leading water fronts are overestimated. Note that in the codes no friction is modelled at the pool bottom and walls.

2) With second-order methods in AFDM, satisfactory results concerning sloshing heights can be obtained; sloshing velocities are overestimated.

3) When the grid is refined, AFDM tends to overestimate sloshing heights. This is because AFDM neglects viscosity terms. The inherent numerical dissipation may become smaller than the physical one. The addition of simple viscosity terms as in SIMMER-II is intended for the SIMMER-III code which is otherwise based on the AFDM numerical scheme.

4) Time-step sensitivity studies reveal no influence on the AFDM and only a minor influence on the SIMMER-II liquid mass distributions.

5) With first order methods not only the sloshing peaks are underestimated but the wave packages are smeared out. This can be drastically seen in Fig. 10.1 and Fig. 10.2 where an AFDM and a SIMMER-II volume fraction plot of the Test Problem 2 are displayed. As can be seen from the second picture of the lower row in AFDM the converging wave package sticks together while in SIMMER-II the converging water is smeared out. IVA3 gives similar results as

SIMMER-II. For better quantification, reassembly rates were further analyzed comparing the SIMMER-II and AFDM results. In Fig. 10.3 the liquid mass distribution of Test problem 2 within the radius (volume) of the original water column is given. From Fig. 10.3, it is obvious that the assembled masses are significantly higher (40 %) in second-order AFDM than in SIMMER-II. The AFDM results slightly overestimate the experimental sloshing heights. Both codes AFDM and SIMMER-II overestimate sloshing velocities by approximately 10 to 20 % compared to the experimental values.

This smearing out of the wave package when using first order methods has the following consequence:

The underestimation of local fuel mass accumulation in the pool center (while at the same time the compaction velocities are slightly overestimated) means for SIMMER-II an underestimation of the neutronic feedback (reactivity ramp rate) in the case of sloshing pool simulation. In /9/ an estimate is given that reactivity ramp rates can be underestimated by a factor of $< 2$.

One must state again that a code which is intended to describe the transition phase behaviour of a core disruptive accident (in the LMFBR field) must be able to model sloshing pool behaviour sufficiently accurate. As a consequence of the analyses given in /9/ it was decided to use higher oder differencing for the future SIMMER-III code which is under development at PNC (Power Reactor and Nuclear Fuel Development Corporation) in cooperation with KfK and AEA-T.

IVA3 which has first order differencing is used in the framework of PWR accident analyses and the neutronic feedback aspect is therefore of minor importance. However the fuel mass distribution during sloshing is not calculated correctly.
The artificial diffusion of mass and the strong smearing may additionally lead to erroneous interactions when simulating the contact between hot and cold fluids (e.g. fuel/coolant interactions). The use of second order methods only brings a gradual improvement in an Eulerian mesh grid. A decisive improvement would be the tracking of surfaces within each cell.

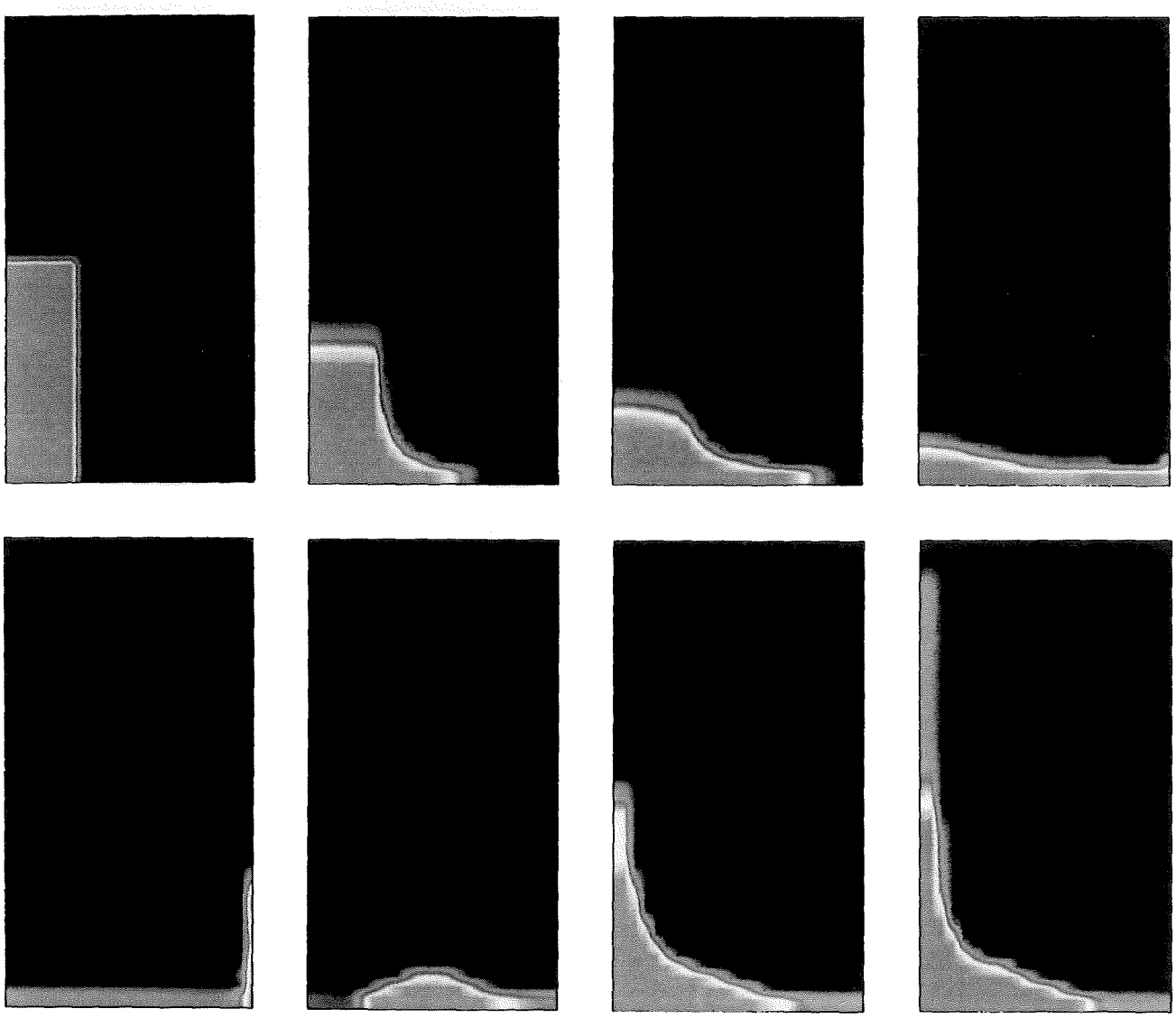

Figure 10.1: Volume fraction plots of an AFDM calculation of Test Problem 2

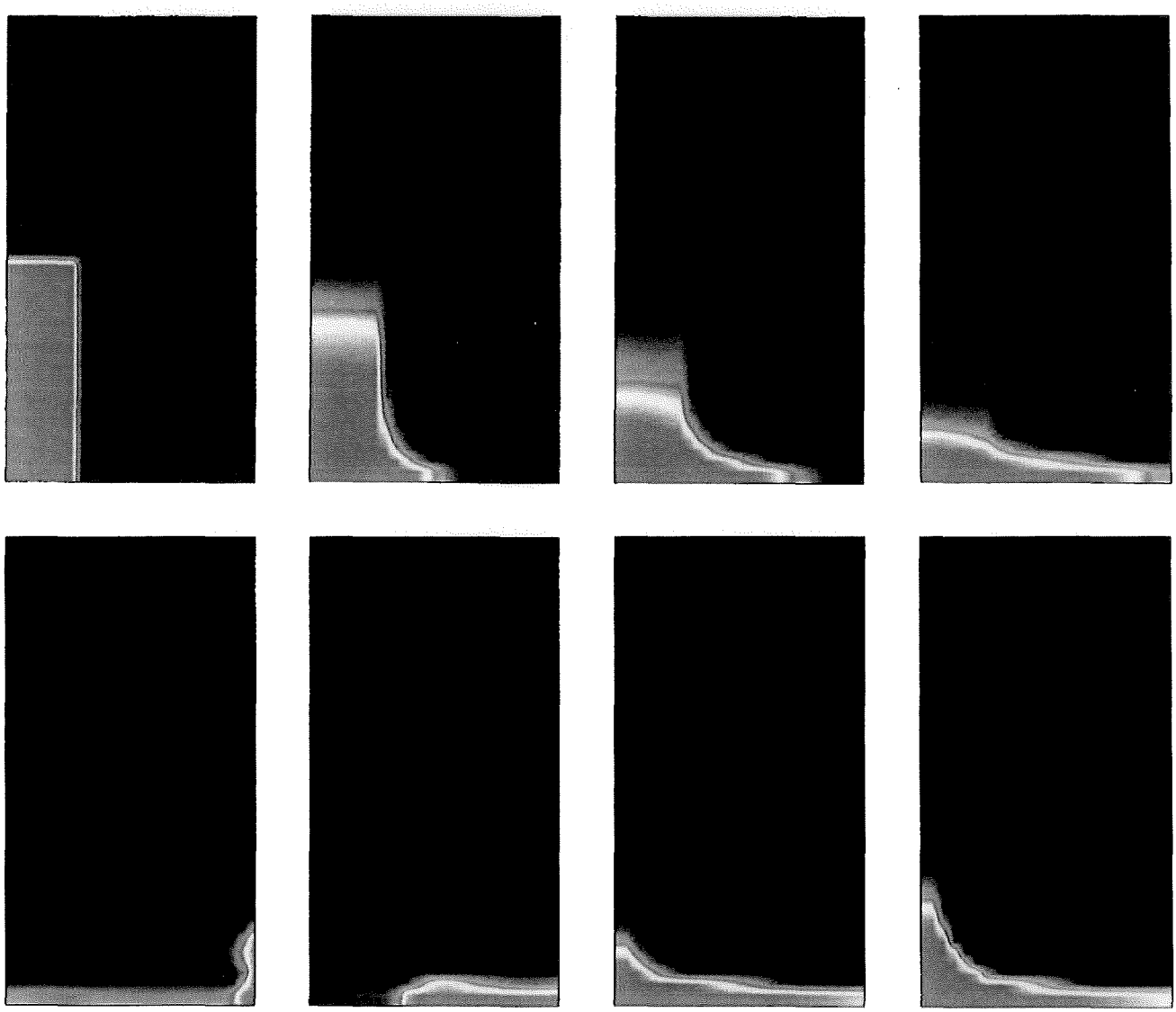

Figure 10.2: Volume fraction plots of a SIMMER-II calculation of Test Problem 2

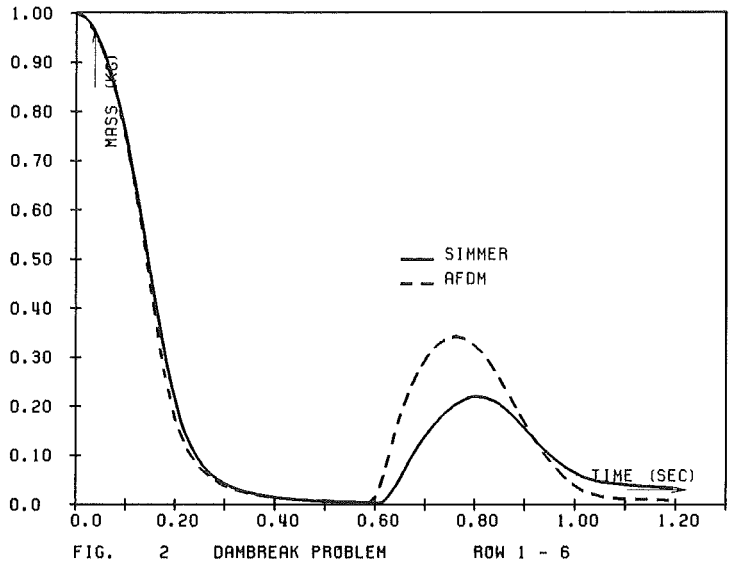


Figure 10.3: Relative liquid mass distribution (out- and in-slosh) in the area of the original water column

## 11. References

/1/ R.M. Cooper
Dynamics of Liquids in Moving Containers
ARS Journal, Vol 30, No. 1, 725 (1960)

/2/ R.L. Bass III, E.B. Bowles, P.A. Cox
Liquid Dynamic Loads in LNG Cargo Ships
SNAME Transaction Vol. 88, 103 (1980)

/3/ H. Hashimoto, S. Sudo
Violent Liquid Sloshing in Vertically Excited Cylindrical Containers
Experimental Thermal and Fluid Science Vol. 1, 159 (1988)

/4/ W.R. Bohl:
Some recriticality studies with SIMMER-II
Proc. Int. Mtg. Fast Reactor Safety Technology, Seattle, August 1979, Vol. 3, p. 1415

/5/ W. Maschek et al.:
Transition phase and recriticality analyses for a SNR-type homogeneous core with the SIMMER-II code
Proc. LMFBR Safety Topl. Mtg., Lyon, July 1982, Vol. 3, p. 357

/6/ S. Kondo et al.:
SIMMER-II application and validation studies in Japan for energetics accommodation of severe LMFBR accidents
Proc. Int. Topl. Mtg. Fast Reactor Safety, Knoxville, April 1985, Vol. 1, p. 481

/7/ T.G. Theofaneous, C.R. Bell:
An Assessment of CRBR Core Disruptive Accident Energetics
Nucl. Sci. Eng. 93, 215 (1986)

/8/ W. Maschek
A Brief Review of Transition Phase Technology
KfK 3330 (1982)

/9/ W. Maschek, C.D. Munz, L. Meyer
Investigations of Sloshing Fluid Motions in Pools related to Recriticalities in Liquid-Metal Fast Breeder Reactor Core Meltdown Accidents
Nucl. Techn. 98, 27 (192)

/10/ L.L. Smith et al.:
SIMMER-II: A Computer Program for LMFBR Disrupted Core Analyses
NUREG/CR-0453, LA-7515 M, Rev. (June 1980)

/11/ W.R. Bohl et al.:
Computational Methods of the Advanced Fluid Dynamics Model
Int. Top. Meetg. on Advances in Reactor Physics, Mathematics and Computation, Paris 1987, Vol. 3, p. 1625

/12/ N.I. Kolev:
A Three-Field Model of Transient 3D Multi-Phase, Three Component Flow for the Computer Code IVA3, Part 1: Theoretical Basics: Conservation and State Equations, Numerics, KfK 4948, Sept. 1991, Kernforschungszentrum Karlsruhe

/13/ N.I. Kolev:
A Three-Field Model of Transient 3D Multi-Phase, Three-Component Flow for the Computer Code IVA3, Part 2: Models for the Interfacial Transport Phenomena Code Validation, KfK 4949, Sept. 1991, Kernforschungszentrum Karlsruhe

/14/ N.I. Kolev:
IVA3: Computer Code for Modeling at Transient Three-Dimensional Three-Phase Flow in Complicated Geometry, KfK 4950, Sept. 1991, Kernforschungszentrum Karlsruhe

/15/ S. Kleinheins:
Internal KfK Report, unpublished

/16/ W. Maschek, A. Roth, M. Kirstahler, L. Meyer
Simulation Experiments for Centralized Liquid Sloshing Motions
KfK 5090 (1992)

/17/ J.J. Stoker:
Water waves
Interscience Publishers, New York 1957